Geomorphology 446 (2024) 108997

Contents lists available at ScienceDirect

Geomorphology

journal homepage: www.journals.elsevier.com/geomorphology

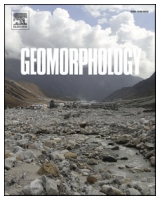

# Historical vertical ground movements in the Campi Flegrei volcano: A new transect across the caldera rim

Gaia Mattei [a], Claudia Caporizzo [a,*], Aldo Cinque [b], Gerardo Pappone [a], Alessia Sorrentino [a], Salvatore Troisi [a], Pietro Patrizio Ciro Aucelli [a]

[a] Department of Science and Technology, Università degli Studi di Napoli Parthenope, Centro Direzionale Is. C4, 80121 Naples, Italy
[b] Department of Earth Science, Environment and Resources, Università degli Studi di Napoli Federico II, Largo San Marcellino, 10, 80138 Naples, Italy

ARTICLE INFO

*Keywords:*
Coastal changes
Bradyseismic crisis
Volcanic areas
Relative sea-level changes
Vertical ground movements
Marine geomorphological surveys

ABSTRACT

This research focuses on a geoarchaeological study of the coastal sector extending from Fusaro coastal lake to Punta Pennata Islet, located in the western peripheral area of Campi Flegrei Caldera (Gulf of Pozzuoli, Italy), to reconstruct relative sea-level (RSL) oscillations and related vertical ground movements which have occurred since the Roman period. Campi Flegrei Caldera is characterized by sudden vertical ground movements of volcano-tectonic origin (i.e. bradyseismic crisis) which strongly modified the coastal landscape during the Holocene. Despite this, the area has been densely inhabited since the Greek-Roman times, preserving numerous traces of its ancient splendor. Part of these findings can be interpreted as high- or low- precision sea-level markers, helping in the reconstruction of the RSL change history. By using a multi-technique approach made of both direct and indirect surveys, the latter performed at the key-site of Punta Pennata through the use of an unmanned surface vessel prototype (ARGO), we investigated different archaeological sites with a twofold purpose. We reconstructed the RSL change of the study area during the last 2.1 ka and, by comparing the RSL data with site-specific geophysical models, we demonstrated that during the considered period the area went through five different evolutive phases characterized by an alternation of prevailing uplift, stability, and subsidence of volcano-tectonic origin, bringing the RSL from −4 and +5 m MSL, up to its current elevation. Moreover, by comparing the RSL data with the present-day sea level, we observed a differential overall subsidence of almost 1-m between the inner and outer sectors of the caldera at Miseno Cape. This validated the presence of a fault, crossing the promontory in an NNW-SSE direction, previously mentioned by other authors. Moreover, the integration of our data and historic sources enabled reconstructing the palaeo-environmental scenario of this area during the 1st century BC.

## 1. Introduction

Volcanic areas are prone to rapid and complex patterns of sea-level change related to the combined effects of global sea-level rise and local subsidence of volcano-tectonic origin (Gunther, 1913; Morhange et al., 1999, 2006; Aucelli et al., 2020, 2021; Mattei et al., 2022). These phenomena can produce local vertical displacement up to several meters with the direct consequence of extensive coastal flooding.

As a result, the vulnerability of coastal zones in volcanic areas is affected not only by the eruption hazard (Santacroce et al., 2003; De Vivo, 2006; Aucelli et al., 2017b; Kennedy et al., 2018), but also by repeated emersion and submersion caused by continuous non-eruptive caldera inflation and deflation (Cinque et al., 1997, 2011; Morhange et al., 2006; Romano et al., 2013; Pappone et al., 2019; Vacchi et al., 2019; Ascione et al., 2020; Budillon et al., 2020, 2022).

In this regard, Campi Flegrei caldera (Gulf of Pozzuoli, Italy), known for being one of the most dangerous volcanic areas in the Mediterranean, is a typical example of a coastal sector affected by sudden vertical ground movements (VGMs) of volcanic origin (i.e. bradyseismic crisis, from the Greek words *βραδύς (bradýs)* and *σεισμός (seismós)*, respectively meaning “slow” and “earthquake”) which have produced local vertical displacements over the last 15 ka (Dvorak and Mastrolorenzo,

* Corresponding author.
*E-mail addresses:* gaia.mattei@uniparthenope.it (G. Mattei), claudia.caporizzo@collaboratore.uniparthenope.it (C. Caporizzo), aldocinque@hotmail.it (A. Cinque), gerardo.pappone@uniparthenope.it (G. Pappone), alessia.sorrentino@collaboratore.uniparthenope.it (A. Sorrentino), salvatore.troisi@uniparthenope.it (S. Troisi), pietro.aucelli@uniparthenope.it (P.P.C. Aucelli).

https://doi.org/10.1016/j.geomorph.2023.108997
Received 17 February 2023; Received in revised form 3 November 2023; Accepted 19 November 2023
Available online 25 November 2023

1991; Cinque et al., 1997; Morhange et al., 1999, 2006; Bellucci et al., 2006; Todesco et al., 2014; Aucelli et al., 2020, 2021; Marino et al., 2022; Orsi, 2022).

Despite its high volcanic risk, the area has been densely inhabited since the Greek and Roman periods and the traces of this dense occupation are still visible along its coasts. In particular, along the submerged sector of Campi Flegrei caldera and its surroundings, the relicts of several luxurious Roman maritime villas lie on the seabed, perfectly preserved, at variable depths between −2 and −6 m MSL due to a volcano-tectonic subsidence occurred in the post-Roman period. These huge complexes of coastal buildings were enriched by fine decorations, thermal baths, fish tanks, and private harbours with piers. Part of these findings can be interpreted and measured as sea-level markers of high or low accuracy depending on the type of indicators. Specifically, in the case of high-resolution markers, a quantifiable relationship between the archaeological feature and former sea-level can be precisely defined (Leoni and Dai Pra, 1997; Lambeck et al., 2004, 2018; Galili et al., 2005; Scicchitano et al., 2008; Morhange et al., 2006; Morhange and Marriner, 2015; Antonioli et al., 2007, 2011; Auriemma and Solinas, 2009; Aucelli et al., 2016, 2019, 2020; Mattei et al., 2018a, 2020). Importantly, many of these structures (and hence the position of former sea-level) can be accurately dated on the basis of detailed information about the villas (Lafon, 2001) and their owners which is contained in epigraphic sources (D'Arms, 1970).

In this study, we applied a multi-method approach to reconstruct past RSL change and VGMs (Giordano, 1995; Quinn et al., 2005; Aucelli et al., 2017a; Mattei et al., 2018a,b; Ferentinos et al., 2020; Caporizzo et al., 2021a, 2021b; Georgiou et al., 2021) on the western rim of the Neapolitan Yellow Tuff (Deino et al., 2004) caldera using the aforementioned archaeological structures. This builds on previous studies of

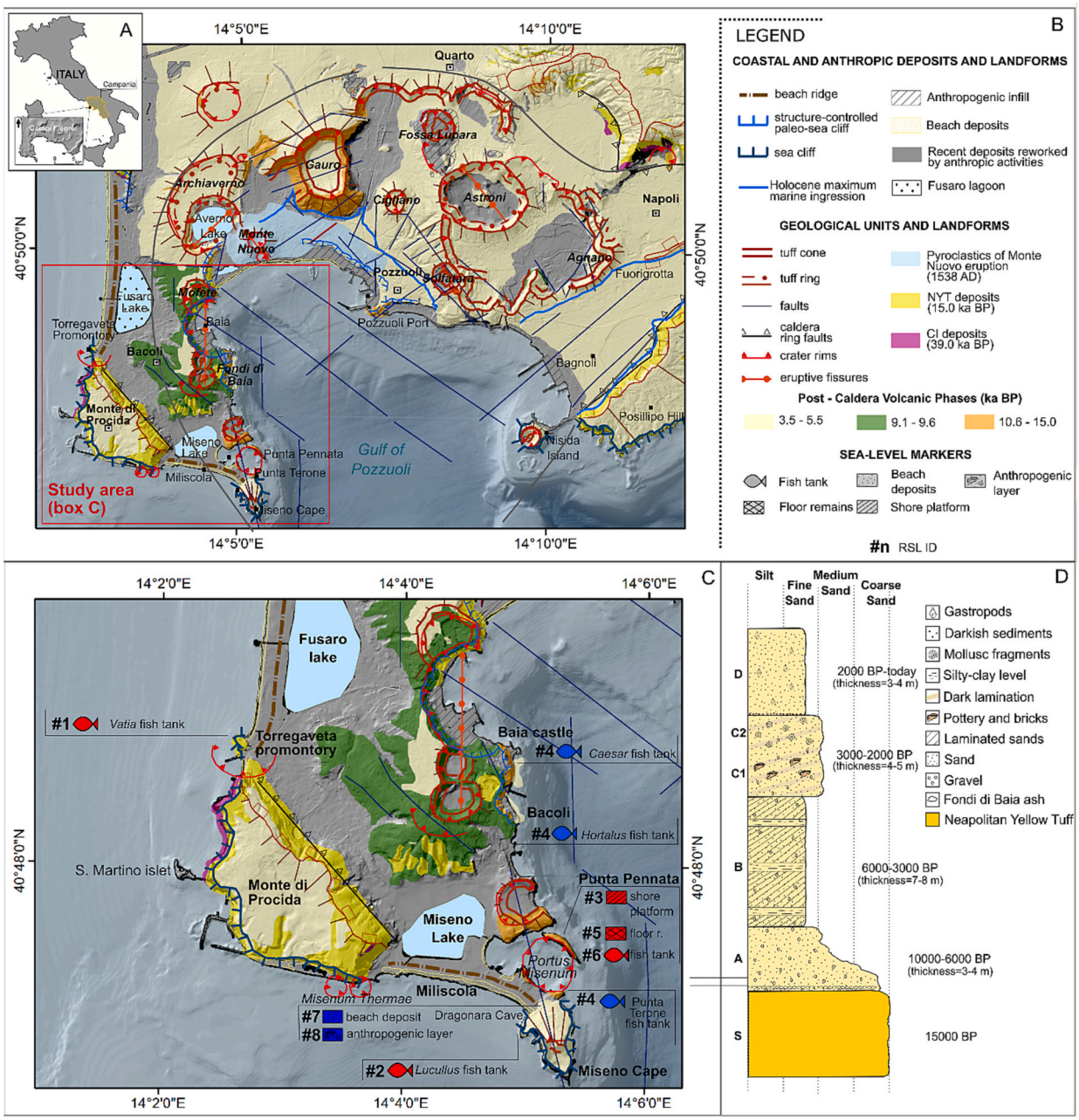


**Fig. 1.** (A) Location map of the study area. (B) Geological and geomorphological sketch of Campi Flegrei Caldera and its surroundings (after CARG; Di Vito et al., 2016). (C) Study area and location of the investigated archaeo-sites. In blue the SLMs from literature, in red the new ones. (D) Stratigraphic succession of the Fusaro coastal lagoon (modified from De Pippo et al., 2007). The basemap was obtained by elaborating LIDAR data provided by the Italian Ministry of Environment.

RSL change and tectonic movements in the wider Campi Flegrei area (e.g. Romano et al., 2013; Russo Ermolli et al., 2014; Di Donato et al., 2018; Pappone et al., 2019; Vacchi et al., 2019; Mattei et al., 2018a; Mattei et al., 2020). We focused on this particular sector of the caldera because it has been only partially studied until now despite the presence of extensive archaeological remains (De Pippo et al., 2007). Our results provide new evidence to supplement existing RSL reconstructions for the study area, further refining the understanding of RSL change in this tectonically complex area. This includes both RSL change over time but also differential behavior in VGMs along a radial transept crossing the inner and outer south-western coastal sector of Campi Flegrei caldera rim.

## 2. Study area

### 2.1. Geological and geomorphological setting

Campi Flegrei volcanic area, located within the Gulf of Pozzuoli (SW Italy), is one of the most densely inhabited districts among the whole metropolitan area of Naples, covering an area of about 12 $km^2$ (Di Vito et al., 2016). The poly-calderic structural depression covers an area of about 230 $km^2$ and includes numerous Quaternary volcanic monogenic edifices, suggesting recurrent activity episodes over time (Di Vito et al., 1999; Del Gaudio et al., 2010 and references therein, Fig. 1).

The volcanic history of the area can be divided into pre- and post-caldera activity. The volcanic activity preceding the caldera formation was characterized by three main eruptive events (De Pippo et al., 2002), interspersed with periods of volcanic quiescence. These were the Campanian Ignimbrite (CI) super eruption (40 ka BP; Isaia et al., 2019 and references therein), the eruption of Masseria del Monte Tuff (MMT, 29.3 ka BP; Albert et al., 2019; Isaia et al., 2019), and, finally, the Neapolitan Yellow Tuff (NYT) eruption (15 ka BP; Isaia et al., 2019 and references therein).

The post-caldera activity, which began after a period of inactivity of 2.0 ka following the NYT deposition, was marked by the succession of approximately 72 explosive and effusive eruptions. These events can be divided into three different phases of volcanic activity (Fig. 1, 15–10.6 ka BP, 9.6–9.1 ka BP, and 5.5–3.5 ka BP, respectively; Smith et al., 2011, Di Vito et al., 1999), whose products are characterized by both lava flows and pyroclastic deposits. The most recent phase of volcanic activity started in historical times, after 3.0 ka of quiescence, forming the Monte Nuovo tuff cone in 1538 CE (D'Antonio et al., 1999).

Episodes of volcanic activity were characterized by intense bradyseismic crises (i.e. local rapid uplift or descent of Earth's surface, respectively positive and negative bradyseism) that induced alternate flooding and re-emersion of wide coastal areas. Several authors have interpreted the ground movements of the Phlegrean area as due to an evolving magmatic body extending down to sub-crustal depths that resulted in the last eruption occurred in 1538 CE (Todesco et al., 2003; Di Vito et al., 2016; Fedi et al., 2018; Orsi, 2022). Recent studies on its hydrothermal system demonstrate that recurrent bradyseismic episodes were accompanied by manifest changes in the degassing budget, degassing patterns, and composition of the fumarolic fluids (Chiodini et al., 2022).

VGMs caused by bradyseismic crises which occurred during historical times are evidenced by the remains archaeological structures such as of villas, harbours, and commercial structures presently located several meters below sea level (Cinque et al., 1991; Morhange et al., 2006; Aucelli et al., 2020, 2021). Evidence is also present on land, the best-known being *Lithophaga* holes bored up to 7 m high on the marble columns of the Roman market of Pozzuoli (i.e. *Macellum* or Serapis Temple; Morhange et al., 2006). These indicate initial subsidence in order to submerge the columns and then uplift to raise them to their present position. The most recent bradyseismic activity has taken place in four episodes: 1950–52, 1969–72, 1982–1984, and 2005 to present (Di Vito et al., 2016). Of these, the 1980s bradyseismic episode resulted in a total uplift of 2 m which effects are still nowadays visible in the harbour area in Pozzuoli Harbour.

The focus of this study is on the extreme western rim of the NYT caldera (Fig. 1), incorporating areas both outside (western part of the study area: Torregaveta promontory to Miseno Cape) and inside (eastern part of the study area: Miseno Cape to Punta Pennata Islet) the rim. The eastern part of the study area runs from Punta Pennata Island in the north to Miseno Cape in the south. Punta Pennata is a remnant of the flank of the Miseno volcano and contains the remains of a Roman villa, mostly now vegetation-covered. The headland of Miseno Cape is a 1 km long by 160 m high rocky headland composed of Miseno Cape Tuff (5.0–3.7 ka; Isaia et al., 2016) which defines the limit of the NYT caldera. Several archaeological structures are cut into the sea cliffs around the headland, notably fish tanks at Punta Terone (ID#1 in our interpretations) and that of *Lucullus* into the Dragonara cave (ID#2 in our interpretations, see Fig. 1C for location).

Moving north-westward, a coastal spit almost 2.0 km-long and called Miliscola beach extends W-NW, with a maximum width of about 60 m. The beach is limited to the west by Monte di Procida, a triangular-shaped and NW-SE orientated rocky promontory. The latter, with a maximum height of about 145 m MSL, is the result of the deposition of different types of volcanic deposits mostly represented by the NYT. Along the seacliffs of Monte di Procida, characterized by an average height of about 60 m MSL, older deposits crop out including Miliscola lithosome, Isola di San Martino lithosome and Torregaveta pyroclastics (Upper Pleistocene; Isaia et al., 2016), and Campanian Ignimbrite (40 ka BP; Isaia et al., 2019). North from the rocky promontory of Torregaveta, made of NYT and hosting the remains of the roman *Vatia* Villa with its fish tank (ID#1, location in Fig. 1C), another sandy coastal strip extends northward, flanking the Fusaro Lake for several kilometers. Fusaro Lake, presently a fully enclosed water body bounded by sandy beaches and dune cordons (Cocco et al., 2002), experienced 4 phases of evolution during the Holocene. Enclosure began during the third phase (3-2 ka BP) when coastal spits joined together and closed the lagoon, probably stabilized by a dominant longshore current coming from the North that firstly formed a dune cordon between the Volturno River and Cuma and, later, between Cuma and Monte di Procida (Brun et al., 2002; De Pippo et al., 2007). The stratigraphic evidence (Fig. 1D; De Pippo et al., 2007) shows 4–5 m of well-sorted medium-to-fine sands, with the frequent presence of a dark lamination, indicative of lagoon sedimentation (unit C1; see Fig. 1D) and, in the upper part, a fining upwards sequence of 5 m of sands, rich in shells with a weak lamination attributable to the coastal spit (unit C2; see Fig. 1D).

### 2.2. Archaeological and historical setting

The area stretching from Fusaro Lake to Miseno Cape - Punta Pennata, passing through Torregaveta, was densely inhabited during the Roman period thanks to the fertility of its soil and despite the proximity of Campi Flegrei.

A crucial event marking the Phlegrean area as an economic power was the transfer of the military fleet from *Portus Julius*, located further east, to the naturally sheltered bay of Miseno (*Portus Misenum* in Fig. 1C, Benini and Lanterni, 2010; Soricelli et al., 2010) between the 1st century BCE and the 1st century CE (Iliano, 2017). The Miseno Roman port (*Portus Misenum* in Fig. 1C) is nowadays totally submerged. The remains of the former quay are submerged on the seabed between −3 to −5 m MSL, located at a maximum of 50 m from the present shoreline, and extend over a length of c. 550 m (Benini, 2007; Benini and Lanterni, 2010). While the innermost part of the bay consisted of a flat sandy beach on which warships could be easily and safely moored, inside the harbour there were piers useful for unloading. The port was composed of two communicating basins separated by two lines of piers in *opus caementicium* (Roman concrete) located at the foot of Punta Pennata, Punta Sarparella, and Punta Terone, with a system of tunnels connecting the inner and outer part of the bay (Benini and Lanterni, 2010; Iliano, 2017).

Across the harbour and the outer tunnel, under Punta Pennata, a line of piers formed the northern arm of the main breakwater of the naval base. Originally, the gallery was accessed via a footbridge to the piers (Maiuri, 1963; Paget, 1971; Iliano, 2017). Into the port, the remains of a fish tank (ID#4, Aucelli et al., 2021) related to a maritime villa coeval with the construction of the military port of Misenum (12 BCE), is carved directly into the Punta Terone promontory. According to Varro (De Re Rustica III, 37 BCE) and Columella (De Re Rustica XVII, 30 AD) this fish tank belongs to *ex petra excisae* category.

On the other side of the bay, a corresponding mole is still visible, ending near the modern lighthouse in the centre of the harbour mouth. In the NW and SE sectors of Punta Pennata islet, several archaeological structures in *opus reticulatum, opus latericium*, and *opus vittatum* represent the remains of a huge maritime villa built in the first years of the 1st century CE (ID#5) and restored in the 2nd century CE (ID#6, Borriello and d'Ambrosio, 1979). To the southeast of the islet, along the ridge, there is a large area with abundant remains of cocciopesto flooring, probably interpreted as a cistern.

Along the western sector of Miseno cape, several remains of a huge maritime viila belonging to Lucullus, with its *ex petra excisae* fish tank (ID #2), are still visible few meters below the MSL (Benini et al., 2008).

To the northwest of Miseno Cape, after the sandy stretch of Miliscola (see Fig. 1 for location), the NYT seacliff at Torregaveta was partly modified by anthropic interventions during the Roman period. The eastern footslope of the promontory is bordered by a platform, probably modeled by anthropic activities, with a depth in its central part varying from about −0.8 m to −0.4 m. Northwards, the coast becomes shallow and hosts a Roman villa, whose construction is attributed by Seneca (*Epistula, LV, 2*) to the Roman consul *Publius Servilius Vatia Isauricus* around the second half of the 1st century BCE (ID#1, Caputo, 2006).

In the northernmost part of the study area, additional details on the isolation of Fusaro lagoon after the 1st century BCE come also from historical sources. These allow refinement of the timing of lagoon isolation evidenced by the sedimentary succession described in the previous section (Fig. 1D). The sources place the formation of the dune cordon to a 40-year period between Strabo's description of the *Acherusia Palus* (ancient name of Fusaro Lake) (Maiuri, 1983) as "a muddy spill of the sea" (Strabo, Geography, V book) in 20 CE and the visit of Seneca in 60–65 CE, who described a coastal spit with a narrow passage laying between the coastal lagoon and the open sea (Seneca, Epistulae ad Lucilium LV).

## 3. Methods

The study area was surveyed by using direct and indirect methods in order to reconstruct the main morpho-evolutive phases that affected the area in the last 2.1 ka. Direct measurements of the depth of archaeological features which represent markers of former sea level were taken by scuba divers at each archaeological site along the inner and outer western coastal sector of Campi Flegrei volcanic area. At the key site of Punta Pennata, these were coupled with underwater remote sensing surveys, comprising acoustic (Sidescan Sonar - SS and Single Beam Echosounder - SBES) and optical (photogrammetry) techniques and optical measurements.

### 3.1. Underwater remote sensing surveys

Indirect investigations were performed by using a prototype of marine drone ARGO - USV (Unmanned Surface Vessel, Fig. 2; for technical detail see Mattei et al., 2018a,b), which is equipped with acoustic and

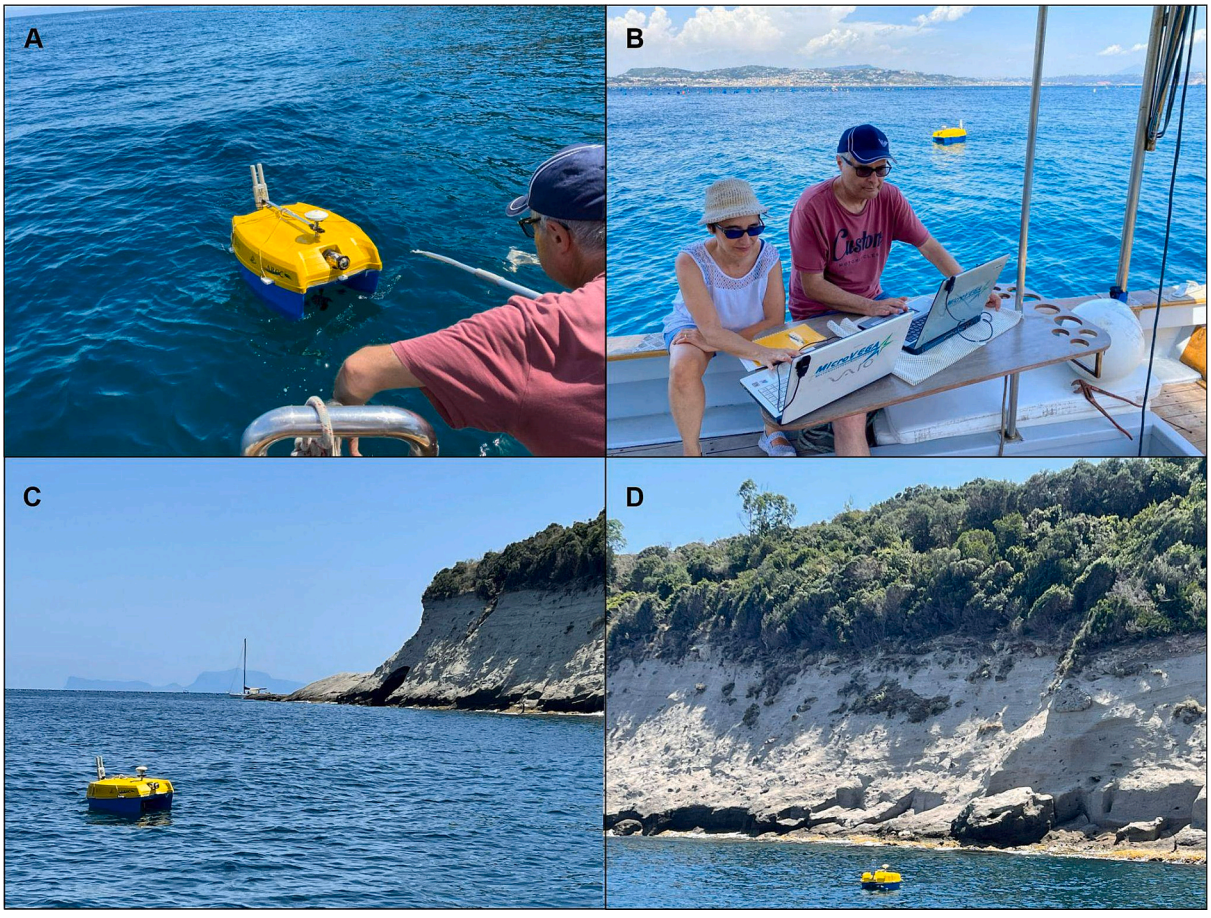


**Fig. 2.** ARGO in action.

optical sensors and designed to investigate very shallow-water sectors characterized by the presence of submerged archaeological structures (Fig. 2; for technical detail see Mattei et al., 2018a,b, Ciaramella et al., 2021). The collection of acoustic data (SBES, SSS) allowed seabed mapping, geomorphological characterization, and archaeological feature detection; optical data (still and video imagery) was processed using Structure-from-Motion (SfM) photogrammetry in order to obtain 3D models of underwater archaeological structures.

ARGO was deployed only at one key site, Punta Pennata. The NW-SE oriented 13 navigation lines have a length of 2900 m and a spatial distance of 2 m.

The SBES installed onboard of ARGO was an Ohmex SonaLite with 200 kHz acquisition frequency mounted on the base of a pole carrying the GNSS antenna. The SSS was a Tritech Starfish 450C with a 450 kHz CHIRP operating frequency. The transducer was embedded in the hull of the USV and offset horizontally from the GNSS antenna by a few centimetres. Position fixing and motion referencing for the SSS and SBES were provided by the RTK GNSS module Emlid Reach M2 and the AltIMU-10 v5 Gyro (accelerometer, compass, and altimeter).

All SBES depths were corrected with respect to the hydrometric level taken from the mareographic station in the Port of Naples belonging to the National mareographic network (ISPRA). SBES data points were manually checked and cleaned to remove false seabed detections. After corrections to hydrometric level, the point layer was interpolated into a DTM of the seabed using the ArcGIS tool IDW (inverse distance weighted interpolator) with a spatial resolution of 0.1 m.

All SSS data were acquired with a slant range of 30 m and processed by using Chesapeake Sonar Web Pro 3.16 software to obtain the full coverage backscatter map of the surveyed area (GeoTIFF mosaic). After applying the slat range correction, a Time-Varying Gain (TVG) filter was applied to boost the gain for features located at larger ranges from the transducer. The analysis of the backscattering signal allowed the evaluation of the characteristics of the acoustic reflectors to assist in discrimination between archaeological remains and the rocky sea bottom.

The onboard ARGO photogrammetric system consists of three submerged cameras (two Xiaomi YI Action and a GoPro Hero3). The two Xiaomi YI Action cameras are placed so that their optical axes are vertical and parallel, with a variable stereoscopic base (b) chosen in relation to the bathymetry of the study area. With our camera configuration, we guarantee a minimum cross-sectional overlap of 80 % during the survey. The third camera (GoPro Hero3) is placed with its axis forming an angle of about 30° with the seabed. It acquires data from non-covered sectors. The videos recorded by the two Xiaomi cameras (previously calibrated in an underwater environment close to the study area to achieve the inner orientation parameters, Menna et al., 2015) are synchronised using an acoustic device integrated into the onboard system that emits sound pulses (beeps) at regular intervals, memorized by the cameras' microphones. Frames were extracted from the videos of the two Xiaomi cameras at a rate to ensure at least a 90 % overlap in the direction of USV movement. Then, the images were processed in order to obtain the photogrammetric 3D model of the surveyed archaeological structures. The image alignment procedure was performed by Metashape Professional Version 1.7.1 software, subdividing the videos into several strips to reduce calculation times. For each strip, a dense point cloud was extracted. The different point clouds were subsequently merged into a single cloud using the GCP placed on the seabed and identified on the images of each strip (Troisi et al., 2015). Precise GCP positions were recorded by a scuba diver using a GPS antenna in fast-static mode. GCP measurements were additionally used to scale and georeference the photogrammetric model.

The photogrammetric model was scaled and georeferenced by using the GPS measurement taken during the GPS fast-static survey of the underwater GCPs.

### 3.2. Direct surveys

In the underwater sector of the study area, several geoarchaeological direct surveys were carried out by a team of specialized scuba divers in order to obtain precise 3D measurements of the structural features such as Roman fish tanks, *pilae* (i.e. cubic structures in concrete used as pillars of piers or coastal structure), and pavement remains intended as sea-level markers (SLMs). The topographic surveys were performed by using a GPS antenna (RTK GNSS Emlid Reach M2) mounted on a graduated range pole useful to evaluate the depth of the archaeological elements. In some cases, the depth measurement was also carried out with a depth gauge. The scuba divers were assisted by two surveyors on a support boat with a GIS-GPS cartographic station to compare in real time the positions of the targets with the archaeological reconstruction obtained from the bibliographic sources. These measurements were essential to perform a correct archaeological interpretation of the morphological characteristics of these structures.

### 3.3. RSL and VGMs reconstruction

The SLMs identified in the study area were classified on the basis of their accuracy level into sea-level index points (SLIPs; i.e. high precision sea-level markers) and terrestrial limiting points (TLPs; i.e. low precision sea-level markers), according to international standards (Shennan and Horton, 2002; Engelhart et al., 2009; Rovere et al., 2016; Lorscheid et al., 2017, Fig. 3). A SLIP is a high-precision sea-level marker with a well-defined relationship between the marker itself and the coeval palaeo sea-level (Shennan, 2015; Vacchi et al., 2016), said indicative meaning (IM). It can be divided in: (1) the indicative range (IR), i.e. the elevation range over which the marker formed; and (2) the reference water level (RWL), i.e. the mid-point of the afore-mentioned range (Shennan, 2015; Vacchi et al., 2016). For each SLIP, the total vertical error (or vertical uncertainty, u) has to be calculated according to the following equation (Vacchi et al., 2016):

$$u = (u\_1^2 + u\_2^2 + \ldots + u\_n^2)^{\frac{1}{2}} \quad (1)$$

When it is not possible to define an IR in terms of precise vertical distance from the former sea level, the sea-level marker is classified as either a marine limiting point, if it formed below former MSL, or a terrestrial limiting point, if it formed above former MSL (Rovere et al., 2016).

Archaeological features suitable for use as SLIPs in the study area consist of Roman fish tanks (Fig. 3A; i.e. maritime annexes to luxurious villas used for aquaculture). They were semi-submerged structures connected with the open sea through one or more channels with several structural elements positioned at a specific altitude with respect to the former mean sea level: (1) the *crepidines*, i.e. levels of walkways encircling the tank; (2) the channel system that allows the tidally controlled water exchange with the open sea; and (3) the *cataracta*, i.e. the sluice gate whose upper part was located just above the mean high water (MHW, Lambeck et al., 2004; Auriemma and Solinas, 2009; Evelpidou et al., 2012; Morhange and Marriner, 2015; Fig. 3).

Consequently, a specific minimum elevation was considered for each structure above MSL at the time of its construction, hereinafter defined as functional clearance (FC), and calculated in a different way for each type of SLM. In general, it is very difficult to establish a general value of FC for archaeological features and the interpretations are often based on observations made on the local ancient structures and their typologies. In the case of Evelpidou et al. (2012), a FC between 0.35 and 0.30 m MSL for the top of sluice gate and crepidines was proposed depending on the dimensions of the tanks along the central Tyrrhenian coasts. Instead, in the case of the Campi Flegrei fish tanks (Aucelli et al., 2020, 2021), the lower crepido and the top of the sluice gate were always positioned at the same altitude. Consequently, we attributed to these structural elements the same FC of 0.2 m above the former MSL, taking into account

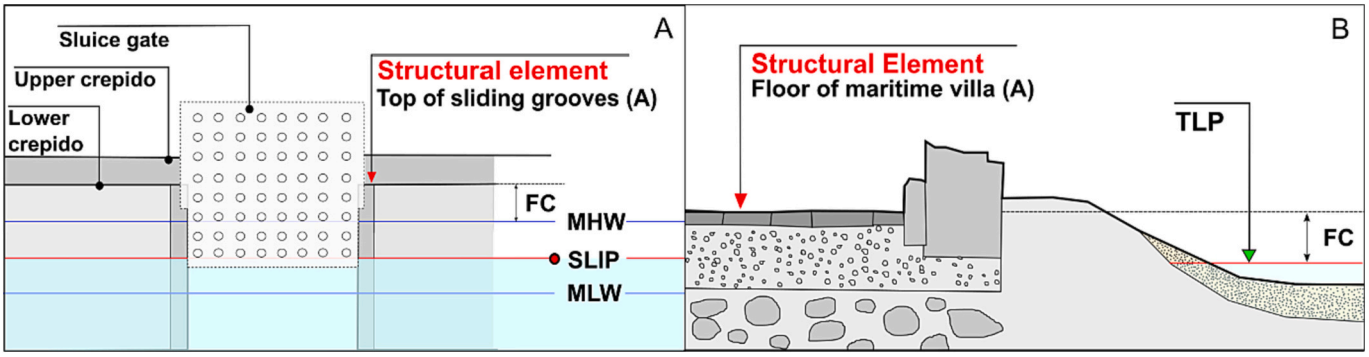


**Fig. 3.** Sketches of (A) A fish tank with lower crepido and sluice gate interpreted as SLIPs. (B) A basal floor of a maritime villa interpreted as TLP. FC is the functional clearance; MHW is the mean high water; MLW is the mean low water.

the dimensions of the tanks. This value is the minimum elevation above the MSL necessary to ensure the water income and exchange with the open sea considering an average height of 1 m for the vertical posts of the sluice gates observed in all of the fish tanks of the Campi Flegrei coastal area.

Therefore, the related determination of the RSL (SLIP) can be evaluated by using the following equation (Aucelli et al., 2021 and reference therein):

$$SLIP = A - FC_{marker} - (MHW - MLW)/2 \quad (2)$$

where A is the submersion measurement of the structural feature corrected with respect to the hydrometric level, in our case taken from the mareographic station in the Port of Naples belonging to the National mareographic network (ISPRA).

Archaeological remains originally built above MHW can also be interpreted as TLPs (Fig. 3B) with a variable FC calculated by considering the original purpose of the structure and the minimum height needed to minimize the risk of flooding by storm waves and groundwater penetration given the characteristics of the local wave and storm climate (Sivan et al., 2001; Auriemma and Solinas, 2009). The values of the FCs considered in this study are specified in the Results section.

Dating of each archaeological structure interpreted as a sea-level marker was obtained from historical sources and specific archaeological studies (cited in the Results section) that describe details attributable to a specific period such as the construction technique or the name of the owner.

RSL changes evidenced from the above archaeological features reflect the combined contribution of local VGMs driven by bradyseism as well as broader changes in sea-level driven by glacio-hydro-isostatic adjustments (GIA). GIA regulates the response of the solid Earth and of the geoid to the melting or accretion of continental ice masses. The GIA-driven RSL changes are described by the gravitationally self-consistent sea-level equation (SLE). Solving the SLE for a prescribed ice-sheets chronology and solid earth rheological model (Spada and Stocchi, 2007), yields the regionally varying RSL change over time. The latter strongly depends on the rheological parameters that define the solid Earth model which is assumed to be spherically symmetric, self-gravitating, rotating, radially stratified and characterized by linear Maxwell viscoelastic layers. A suite of RSL curves was produced for the study area (Mattei et al., 2022) by using the ICE-5 G (Peltier, 2004), ICE-6 G (Peltier et al., 2015) ice sheet chronologies and the ANICE-SELEN coupled ice-sheet - sea-level model (de Boer et al., 2013, 2014). The SLE has been solved for a total of 54 models (3 ice-sheets chronology x 6 mantle viscosity profiles x 3 lithosphere thickness), assuming three values of lithosphere thickness, respectively of 60 km, 90 km and 120 km, and considering values for the lower and intermediate mantle viscosity ranging between 2–10, 0.5–1 and 0.2–0.5 Pas, respectively.

Therefore, in order to assess the overall vertical ground movement (VGM), intended as the sum of positive and negative landmass movements occurred in the last 2.1 ka, we adopted a Bayesian statistical approach based on the use of Monte Carlo simulations (Mattei et al., 2022). The method involved a comparison between the observed sea-level positions ($RSL_O$) and those predicted by GIA models for the same age ($RSL_P$):

$$VGM_n = RSL_{On} - RSL_{Pn} \quad (3)$$

where n is equal to 1000.

Moreover, we also evaluated the amount of vertical ground movements occurred between a morpho-evolutive phase and another (partial VGM) in order to detect and measure the vertical trend reversal.

## 4. Results

Surveys were performed in 3 coastal areas, all characterized by the presence of chronologically well-constrained archaeological remains. These areas are: 1) the rocky coasts of the Torregaveta Promontory, 2) Miseno Cape, and 3) Punta Pennata Islet.

### 4.1. Torregaveta Promontory

At the foot of the tufaceous promontory of Torregaveta, the remains of a Roman maritime villa are located to the north of Torregaveta Dock (Fig. 4A; see location in Fig. 1). The villa and its fish tank (Fig. 4B) were historically attributed by *Seneca* (*Epistula, LV, 2*) to the console *Publius Servilius Vatia Isauricus*, in charge for the year 79 BCE, and consequently dated to the first half of the 1st century BCE (Caputo, 2006).

During the direct survey carried out at this site, the remains of the fish tank including a well-preserved lower crepido (Fig. 5A) were detected. The present submersion depth of the crepido was measured at −2.9 m MSL. This gives a SLIP (RSL, ID#1) at −3.3 m for this first half of the 1st century BCE, which, in turn, enables calculation of the calculation of a VGM of −2.56 ± 0.46 m (Table 1). The fish tank, lacking the external wall in which the sluice gate was constructed and characterized by a length and a width of about 8 and 5 m, is carved along the southern border of a sub-horizontal surface sculptured in tuff, which is interpreted as a palaeo-shore platform modified by anthropic interventions such as a rock-cut channel. The platform, about 60-m long and about 65-m wide, covers an area of about 3000 $m^2$ and is cut by a Y-shaped channel NE-SW oriented. The depth of the tufaceous platform is not constant and varies from −0.8 m to −0.4 m in its central part, while the internal and external margins are found respectively at about −0.2 m and −1.0 m of depth. The use of the channels dug on the platform was probably linked to the water supply of the fish tank. Additional measurements were taken from other archaeological structures associated with the villa, in particular at the *nymphaeum* (30 × 40 m, a monument consecrated to the nymphs, especially those of springs). The submersion measurement of the *nymphaeum* floor, located at −1.35 m MSL, was performed on the tufaceous platform on which it was carved, at the base

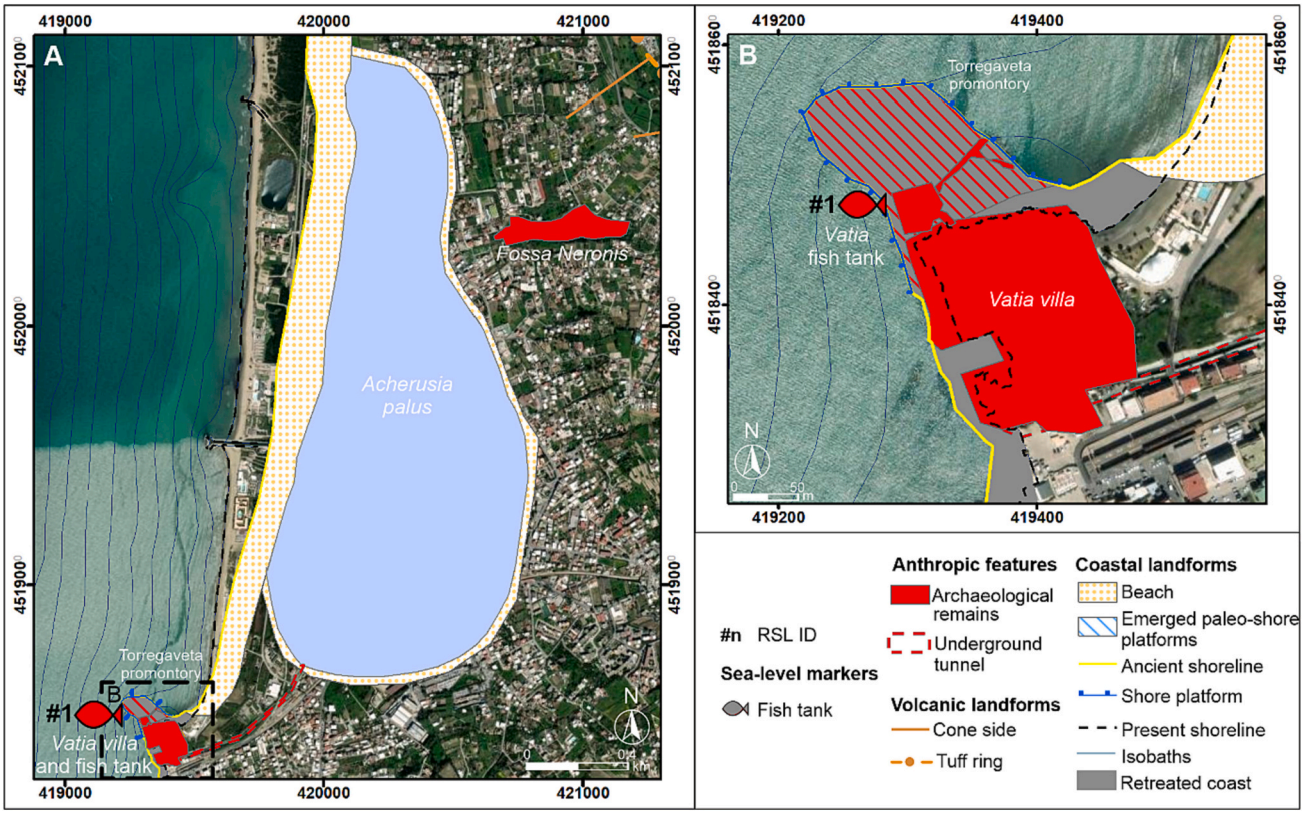


**Fig. 4.** (A) Reconstruction of the Roman coastal landscape at the foot of Torregaveta promontory. (B) Zoom on the investigated archaeological site. In red the new SLM.

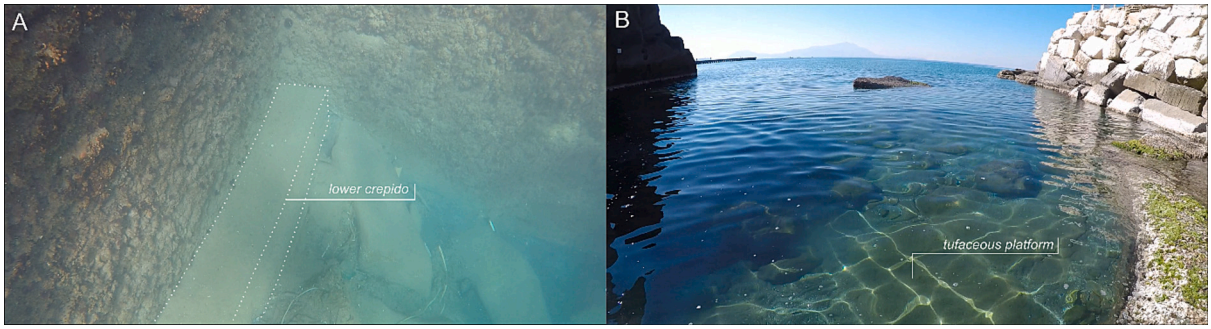


**Fig. 5.** Remains of the *Vatia* Villa at Torregaveta. (A) Detail of the lower crepido detected during the direct survey. (B) Tufaceous platform detected at the base of the apsis of the *nympheaum*.

of the apsis of the *nymphaeum* (Fig. 5B), and interpreted as a TLP. Considering that nymphaea were typically constructed near the sea in order to withdraw water for the functioning of the water features, this measurement was corrected with respect to a FC ranging between 1.0 and 1.5 m and, consequently, an upper limit for the sea-level position during the 1st century BCE was estimated at about −2.7 m MSL.

### 4.2. Miseno Cape

Along the NW side of Miseno Cape, the remains of a fish tanks system are located near the famous Dragonara cave (Figs. 6A and B, and 7A and B; see location in Fig. 1). These fish tanks were historically attributed to the Roman patrician *Lucullus* who was consul in 74 BCE and then moved to Miseno in 60 BCE (Benini et al., 2008). The complex is characterized by the presence of two front entrances (Fig. 7A and B), each measuring about 6 mm in width and 6.5 m in height (Benini et al., 2008). These entrances lead to two square rooms, each roughly 7 m by 6 m in size. These rooms are separated by a partition that is approximately 1.2 m thick. The walls and ceilings of these rooms are made of natural rock, and the floor is currently covered with sand, located at a depth of approximately 3.5 m. At first glance, it appears that these two chambers are independent of each other. However, they are actually connected by an arched passage currently submerged. Inside this passage, the lower level of crepido is located bordering an ancient channel also covered in sand.

During the direct survey at this site, the abovementioned lower level of the crepido (Fig. 7C and D), nowadays located at −2.8 m MSL, was measured (RSL, ID#2). This gives an estimated RSL elevation of −3.2 ± 0.29 m MSL for the second half of the 1st century BCE, from which an overall VGM of −2.47 ± 0.45 m (Table 1) was calculated by the Monte Carlo procedure.

On the opposite side of Miseno cape, a fish tank (Fig. 6), related to a maritime villa coeval with the construction of the military port of *Misenum* in 12 BCE, was already surveyed by Aucelli et al. (2021) and

**Table 1**
Sea-level markers identified in the studied coastal sectors: ID (column 1); type (sea-level index point – SLIP or terrestrial limiting point – TLP; column 2); Type of measured structural features (column 3); Location of the measured structural features (column 4); Age expressed in ka BP (column 5); Age expressed in yr BC/AD (column 6); submersion measurements corrected with respect to the hydrometric level (expressed in meters, column 7); RSL and related uncertainty (expressed in meters, column 8); overall vertical ground movement and related uncertainty (VGM; expressed in meters, column 9); partial vertical ground movement calculated with respect to two chronologically subsequent SLIPs in the outer (from ID#1 to ID#2) and inner (from ID#3 to ID#8) coastal sectors of Campi Flegrei NYT caldera (expressed in meters, column 10); rate of partial vertical ground movement calculated with respect to two chronologically subsequent SLIPs in the outer (from ID#1 to ID#2) and inner (from ID#3 to ID#8) coastal sectors of Campi Flegrei NYT caldera (expressed in millimeters per year, column 11); source of data (column 12).

| ID | Type | Structural feature | Location | Age (ka BP) | Age (yr BC/AD) | Altitude (m MSL) | RSL (m MSL) | VGM (m) | ParVGM (m) | ParVGM rate (mm/yr) | Source |
|---|---|---|---|---|---|---|---|---|---|---|---|
| #1 | SLIP | Fishtank - lower crepido | Vatia Villa | 2.02 ± 0.01 | 79 BCE | −2.9 | −3.3 ± 0.29 | −2.56 ± 0.46 | – | – | New data |
| #2 | SLIP | Fishtank - lower crepido | Lucullus Villa | 2.01 ± 0.01 | 60 BCE | −2.8 | −3.2 ± 0.29 | −2.47 ± 0.45 | −0.09 ± 0.45 | −4.7 | New data |
| #3 | SLIP | Shore platform | Punta Pennata | 2.90 ± 0.6 | 950 BCE | −2.5 | −2.75 ± 0.5 | −1.58 ± 0.73 | – | – | New data |
| #4 | SLIP | Fishtank - top sluice gate | Punta Terone | 2.02 ± 0.05 | 75 BCE | −3.7 | −4.1 ± 0.3 | −3.35 ± 0.44 | 1.77 ± 0.58 | 2.0 | Aucelli et al., 2021 |
| #5 | TLP | Floor remains | Punta Pennata Villa | 1.9 ± 0.05 | 50 CE | −3.0 | < −4 | – | – | – | New data |
| #6 | SLIP | Fishtank - top sluice gate | Punta Pennata Villa | 1.80 ± 0.05 | 150 CE | −1.9 | −2.3 ± 0.3 | −1.65 ± 0.43 | −1.7 ± 0.43 | −7.7 | New data |
| #7 | SLIP | Beach deposits | Miseno Thermae | 1.00 ± 0.15 | 950 CE | 5.0 | 5 ± 1 | 5.34 ± 1.03 | −7 ± 0.73 | −8.7 | Aucelli et al., 2021 |
| #8 | TLP | Anthropogenic layer | Miseno Thermae | 0.85 ± 0.15 | 1100 CE | 2.0 | < 4 | – | – | – | Aucelli et al., 2021 |

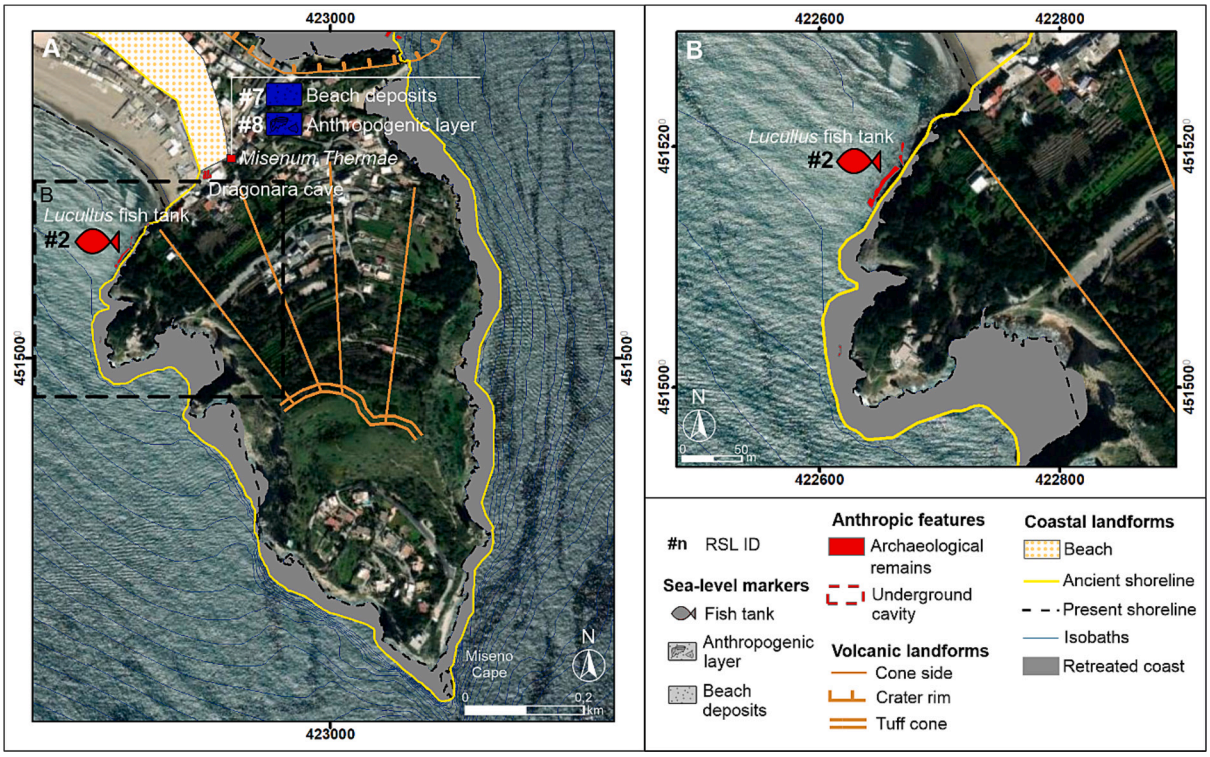


**Fig. 6.** (A) Reconstruction of the Roman coastal landscape along the NW side of Miseno Cape (B) Zoom on the investigated archaeological site. In blue the SLMs from literature, in red the new ones.

interpreted as a SLIP at 4.2 ± 0.2 m (RSL, ID#4 in our interpretations).

### 4.3. Punta Pennata islet

Punta Pennata islet is bordered by a seacliff in well-stratified Miseno Tuff (Fig. 8) with a maximum height of 13 m. At this site, an ARGO survey allowed mapping the underwater coastal landscape (Figs. 9 and 10). This indirect survey detected and enabled characterization of a 50 m-wide platform which is cut into Miseno Tuff and lies submerged on the northern side of the islet, with its inner margin located at a depth of −2.5 m MSL and a slope of about 1° following the strata dipping. By analyzing the backscattering signal of SSS data, the high acoustic reflectivity of the platform demonstrates its rocky nature, in accordance with what was observed during the direct survey. In addition, the calculated high rugosity index represents a piece of evidence of the erosion processes affecting its surface. Consequently, the morphology of the platform, based on the bathymetric information and backscatter data, suggests that it is an erosional landform, likely a shore platform cut

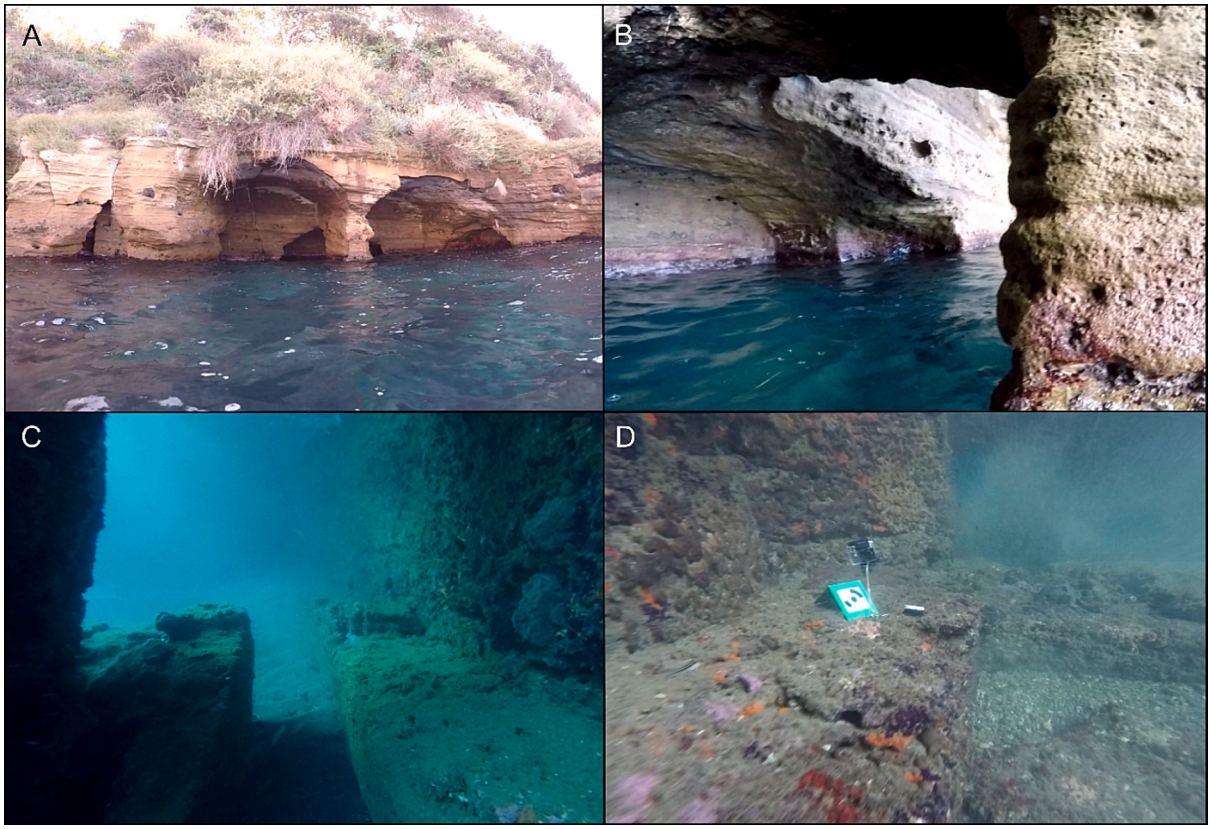


**Fig. 7.** Underwater photos of *Lucullus* fish tank at the Dragonara Cave. (A, B) Emerged part of the fish tanks complex. (C, D) Details of the detected lower crepido.

by wave and/or tidal action. Also present on the platform are archaeological structures, visible on the backscatter as upstanding linear or regular-shaped features. These were also identified during the direct survey and confirmed to include numerous wooden poles, post holes and concrete structures. These archaeological features are the remains of the huge Punta Pennata maritime villa which was built in the first years of the 1st century CE and renovated in the 2nd century CE (Benini, 2007).

The presence of archaeological remains on the platform demonstrates its polycyclic evolution. It was probably initially cut before the Roman period and then during the Roman period was elevated above sea-level by volcano-tectonic uplift whereupon it formed a terrace overlooking the sea, and thus a suitable spot for construction of a luxurious villa.

Furthermore, both the platform and its archaeological structures can be used as sea-level markers. According to several authors (i.e. Tursi et al., 2023 and reference therein), the inner margin of a shore platform (i.e., the contact point between the horizontal bedrock and the vertical rocky cliff) can be interpreted as an SLIP because it is typically positioned at the mean higher high water (MHHW, i.e., average of the higher high water height of each tidal day observed over a Tidal Datum Epoch). In the study area, MHHW is 0.25 m which, when combined with the present inner margin submersion depth (−2.5 m MSL), suggests a first phase of RSL at 2.75 ± 0.5 m MSL during the pre-Roman period (RSL, ID#3). Timing of this phase can be constrained firstly by the stratigraphy of the La Starza marine terrace (eastern side of the Gulf of Pozzuoli: Isaia et al., 2019) which indicates high RSL of up to 50 m at 5.25 ka. Secondly, geoarchaeological measurements taken by Aucelli et al. (2021) along the nearby Baia – Miseno coastal sector suggest that this area was totally emerged during the 4th/3rd centuries BCE when the RSL was not much higher than −8.5 m. Consequently, we can deduce that the shore platform formed in a period of RSL stability happened during a wider phase of uplift that occurred after the 3rd eruptive epoch (5.5–3.5 ka BP, see Section 2.1) and before 2.3 ka BP. The calculated overall VGM is therefore −1.58 ± 0.73 m (Table 1). On the platform, the lowest rooms of the villa, which were built during the 1st century CE, (Figs. 9A and 11) are presently submerged at a depth of about −3 m MSL. Given that they had to be positioned at least 0.5 m above contemporary MSL indicates that during this phase, RSL was lower than −4 to −5 m MSL (RSL, ID#5).

During the 1st century CE the platform hosted the lowest rooms of the Punta Pennata Roman villa (Figs. 9A and 11) that had to be positioned at least 1/2 m above the MSL of that time. Consequently, we can affirm that during the first villa phase (1st century CE) the RSL was lower than −4/−5 m MSL at that time (RSL, ID#5). In this case, according to our procedure, no VGM is calculated for a TLP.

Punta Pennata is crossed by three tunnels positioned in the centre and at the ends of the islet (Fig. 8A and B). The first one in the western sector is partially closed by modern collapses. The second one, in the central part, has a floor at −2.20 m MSL and is connected to the port quay, therefore it certainly emerged up to the 2nd century CE. The third tunnel, at the eastern end, is of larger dimensions and at least six meters deep (Benini, 2007). Northward, an additional SLIP was obtained from a fish tank located on the northern tip of the submerged platform, where two in situ sluice gates 1.4 × 1.4 m in size (see Fig. 9B for the photogrammetric reconstruction) were detected during the direct survey. These remains can be attributed to the second phase of villa construction during the 2nd century CE (Benini, 2007; Fig. 11B). The top of the vertical posts of the best preserved sluice gate was measured at −1.90 m MSL which gives a SLIP at −2.3 ± 0.3 m MSL (RSL, ID#6; Figs. 8F and 9B) and in turn a VGM of −1.65 ± 0.43 m (Table 1).

## 5. Discussion

The data collected so far are interesting not just because they allow the assessment of the RSL change over time and the consequent VGMs but also because they enable us to evaluate the variability of these


**Fig. 8.** (A) Panoramic view of Punta Pennata. (B) Semi submerged tunnel of Roman time. (C, D, E, G) Underwater photos of archaeological remains related to the first constructive phase of Punta Pennata villa. (F) Best preserved sluice gate of the second constructive phase of Punta Pennata villa.

phenomena both within and outside the caldera. This is an important challenge considering that this type of evaluation has never been carried out so far, apart from the evaluation of the present-day VGM trends. In fact, presently, the whole caldera is leaving a phase of uplift, that reaches its maximum value in the central part (Pozzuli port) with a rate of 15 mm/month.

### 5.1. RSL evolution: inside the caldera

The coastal landscape of Miseno - Punta Pennata sector experienced five evolutive phases in the period between the first Roman occupation in the 5th century BCE and the 2nd century CE, according to our surveys and interpretation of bibliographic sources (Benini and Lanterni, 2010; Borriello and d'Ambrosio, 1979). During the first evolutive phase, which occurred before the Roman occupation, the palaeo-shore platform bordering the northern side of Punta Pennata formed, as a result of wave action on the volcano flank, taking place at a RSL stand at $-2.75 \pm 0.5$ m MSL (ID#3, Fig. 12).

This pre-Roman landform can be associated with a similar shore platform located to the north of Punta Pennata, between Baia and Bacoli (Aucelli et al., 2021) on which thermal baths were constructed at the beginning of the second evolutive phase in the 1st century BCE (Di Fraia, 2013). However, the re-emersion of the platform certainly occurred during an uplift phase before 2.1 ka BP (Fig. 12) when the beachface layer at Baia was deposited at $-7.9 \pm 1$ m MSL, according to Aucelli et al. (2021). No evidence was found in Miseno – Punta Pennata sector

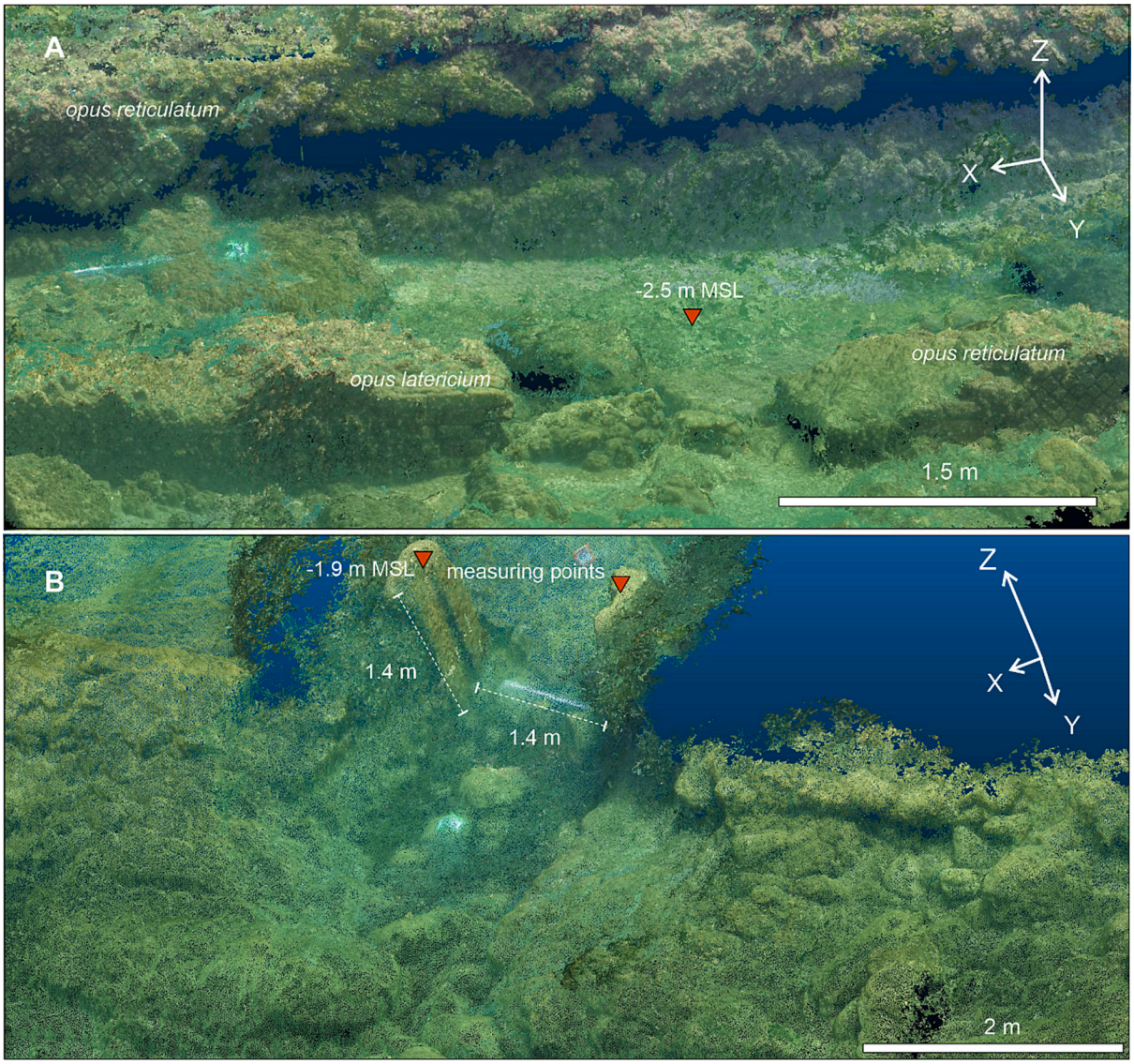


**Fig. 9.** (A) Photogrammetric reconstruction of one of the best-preserved rooms of the first constructive phase of the villa. (B) Photogrammetric reconstruction of the best preserved sluice gate of the fish tank.

concerning this VGM, consequently, we can affirm that the second evolutive did not leave geomorphological or archaeological evidence in the study area. It was certainly followed by subsidence that brought the RSL at −4.1 ± 0.3 m MSL (ID#4, Fig. 12), marking the beginning of the third evolutive phase characterized by the construction of three fish tanks, two north of the study area and one within it (*Caesar, Hortalus*, and Punta Terone fish tanks), positioned along the whole Baia - Miseno sector (Aucelli et al., 2021), which indicates a RSL stand at −4.1 ± 0.3 m MSL (ID#5, Fig. 12) that characterized the third evolutive phase. Therefore, the time span covered by the three fish tanks (first half of the 1st century BCE) appears to be a period of volcano-tectonic stability (Aucelli et al., 2021). This stage lasted until the Augustan Age (i.e. 27 BCE–14 CE), when the Punta Pennata villa was built on the cliff and on the uplifted palaeo-shore platform (RSL, ID#5 in Fig. 12).

The fourth evolutive phase was characterized by subsidence of about 1.7 m at a rate of −7.7 mm/yr (Table 1) that brought the RSL to −2.3 ± 0.3 m MSL (ID#6, Fig. 12), as measured through the fish tank at Punta Pennata, probably constructed during the villa restoration. During the two centuries after (4th evolutive phase), the trend of subsidence accelerated with a rate of −8.7 mm/yr producing the submersion of the whole coastal sector up to 5 m MSL and the consequent deposition of beach deposits on the floors of the *Misenum Thermae* (i.e. Miseno thermal baths, ID#7, Fig. 9; Cinque et al., 1991; Aucelli et al., 2021). A period of uplift totaling 5.34 ± 1.03 m started soon before the Monte Nuovo eruption (1538 CE), (RSL, ID#8;; Table 1) leading the RSL to its current position (fifth evolutive phase; Fig. 12).

### 5.2. Spatial variations in RSL across the caldera rim

The four SLIPs (*Vatia*, Punta Terone, *Lucullus, and Hortalus* fish tanks, Fig. 13) deduced from fish tanks built during the 1st century BCE (location in Fig. 1C) along the whole study area denote a differential behavior between the inner and outer south-western coastal sector of the NYT caldera. In terms of the sum of positive and negative landmass movements occurred in the last 2.1 ka, both coastal sectors were affected by an overall subsidence with variable magnitude (−2.38 and −3.18 ± 0.82 m, respectively), exacerbated by 0.82 ± 0.66 m of glacio-hydro-isostatic adjustment. An ideal transect NNW-SSE oriented and passing through the caldera rim (Fig. 14) shows a 1-m difference in vertical displacement, better constraining the presence of a fault crossing the Miseno promontory, according to previous studies (Di Vito et al., 2016).

This interpretation is substantiated by comparison with RSL

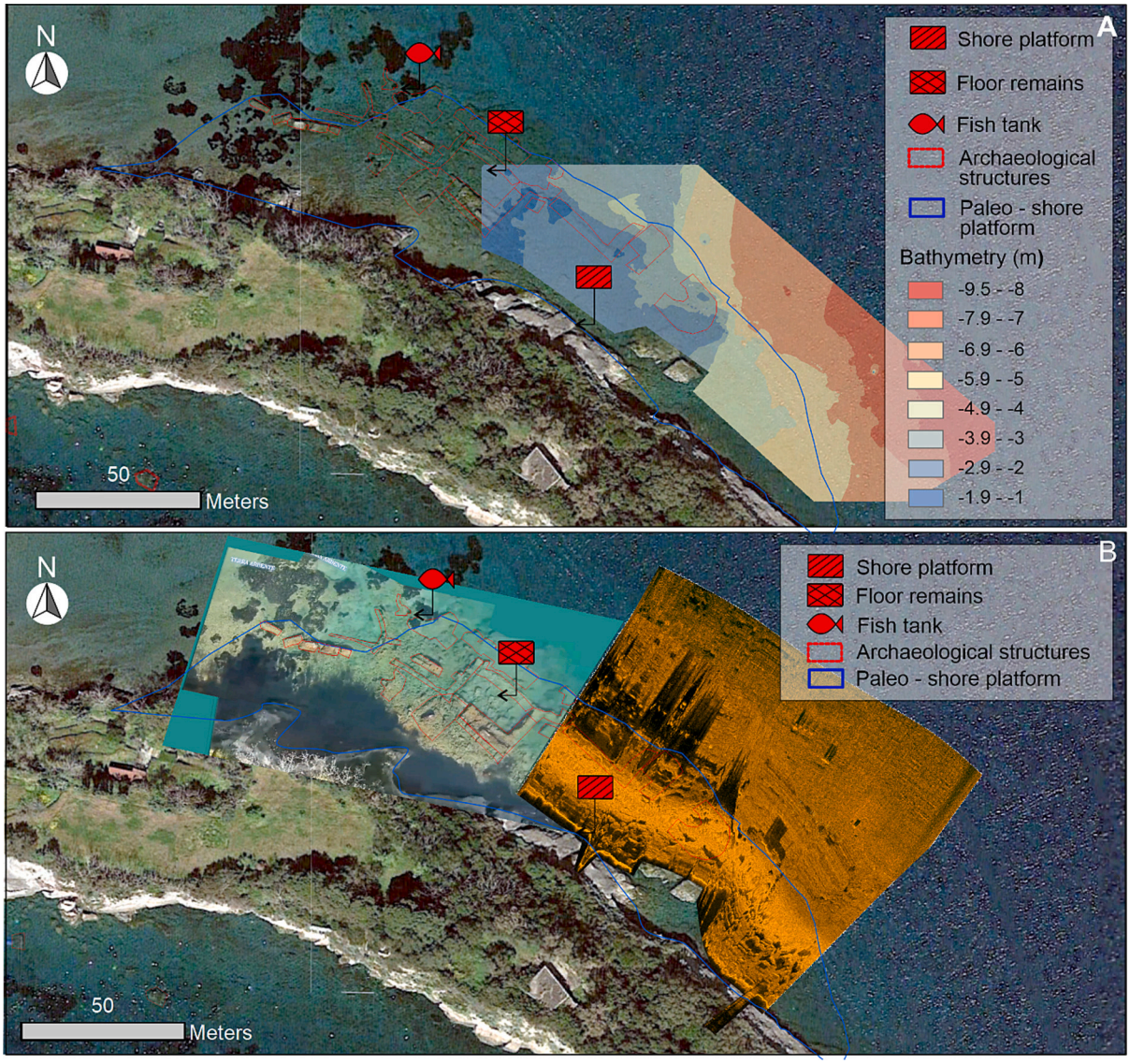


**Fig. 10.** Results of Punta Pennata survey. (A) Bathymetric map obtained from interpolation of SBES data. (B) SSS mosaic and satellite image (Google Earth Pro) with the identification of the submerged archaeological structure.

measurements from the eastern part of the outer rim along the Posillipo coast (Aucelli et al., 2018, 2019; Mattei et al., 2018a,b), where a 1st century BCE RSL stand at −3.2 ± 0.29 m MSL was deduced from the geoarchaeological study of port structures and a fish tank belonged to *Publio Vedio Pollione*.

In terms of coastal changes related to this differential subsidence across the caldera rim, we reconstructed a general progradation of low-lying areas and a retreating trend of the tuff seacliffs (Fig. 13). In particular, after the consolidation of the dune ridge at Fusaro (ancient *Acherusia Palus*) which occurred during the 1st century BCE in accordance with historical sources, the sandy areas of Miliscola and Fusaro itself underwent a progradation of a maximum of ~250 m due to the sedimentary inputs coming from the Volturno River located 30 km to the NW (Fig. 13). In contrast, the subsiding trend induced a progressive coastal retreat of the steeper cliffed and rocky sectors with the total submersion of the uplifted palaeo-shore platforms at Monte di Procida and Miseno Cape (Fig. 10).

## 6. Concluding remarks

This geoarchaeological study mainly concerned a poorly-researched sector of the 15 ka-old NYT caldera of Campi Flegrei (Fig. 1). Namely, we investigated the peninsular area extending from Torregaveta to Miseno Cape, an area where the presence of submerged Roman ruins on both the W and the E coast of the promontory allowed collection of well-dated indicators of ancient RSLs and analysis of the causative VGMs along a section passing radially across the caldera rim. The collected data allowed us to assess the overall vertical trend intended as the sum of positive and negative VGMs occurred within the study area after the Roman period, observing a 1-m difference outside and inside the caldera rim. They also enable the quantification of the VGMs which occurred between the 1st century BCE and 2nd century CE in the portion of the study area falling inside the NYT caldera (area between Miseno and Punta Pennata).

Regarding the area outside the NYT caldera, the fact that post-Roman subsidence has been evaluated can be ascribed to the regional tectonics of the Naples Gulf (a semi-graben characterized by a subsiding trend with a rate of 1 mm/y according to Milia et al., 2003).

In terms of coastal changes, the last 2 millennia were generally characterized by a retreating trend of the coastline due to the submergence caused by glacio-hydro-isostatic sea-level rise and, above all, by the prevailing subsidence trend that lasted 1.5 ka (2.5–1.0 ka BP). The

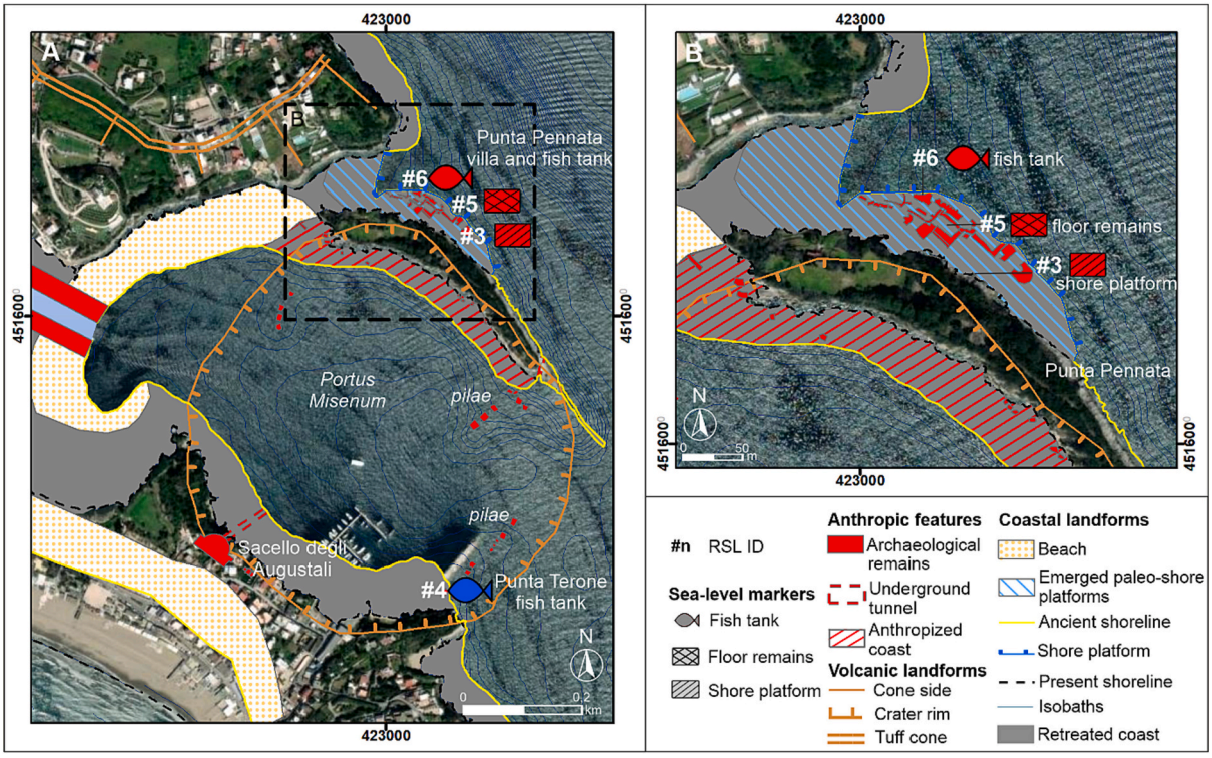


**Fig. 11.** (A) Reconstruction of the Roman coastal landscape at Punta Pennata islet. The term "anthropized coast" implies a coastal sector mainly modeled by anthropic activities. (B) Zoom on the investigated archaeological site. In blue the SLMs from literature, in red the new ones.

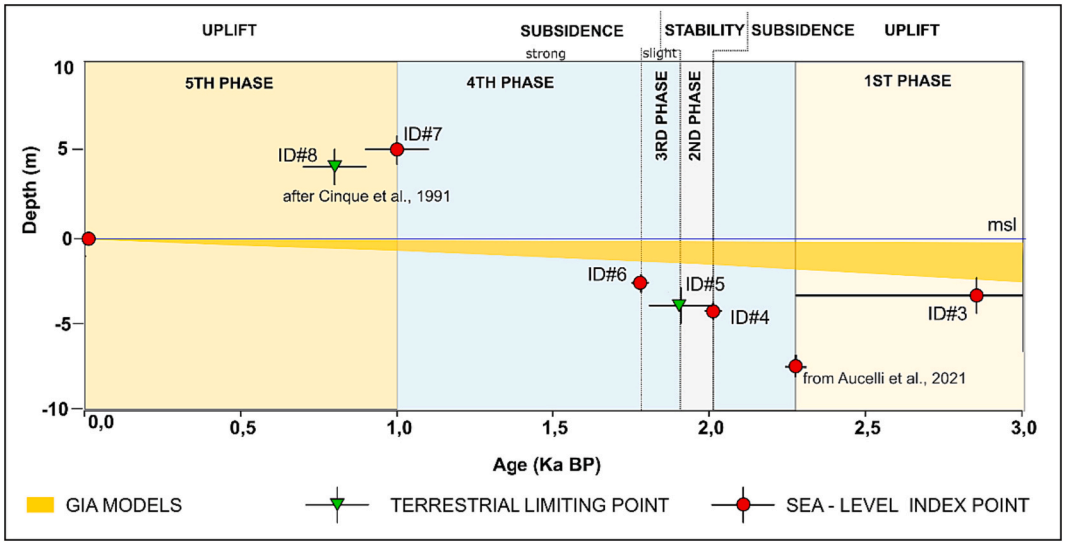


**Fig. 12.** RSL curve deduced from the measurements and bibliographic data at Miseno Cape - Punta Pennata sector. The yellow curve represents all of the area covered by the 54 GIA curves produced by Mattei et al., 2022.

coastline retreated particularly fast at places (e.g. between Baia and Punta Pennata) where the RSL rise flooded some pre-existing palaeo-shore platforms, which had initially formed during the pre-Roman period. A different response characterized the embayed coastal reaches of the study area, where RSL rise was not only compensated but even overwhelmed by coastal progradation. A seaward growth was favoured by the drift of sands from the mouth of the Volturno River and from the much erodible pyroclastic rocks exposed in the bay-side sea cliffs.

In particular, during the 1st century BCE, a period without significant VGMs (Aucelli et al., 2021), the longshore current fed by the Volturno River mouth was able to close the Fusaro lagoon with an extended spit bar, turning it into a coastal lake; a change that was described by the Latin author and politician *Seneca*, as an eyewitness.

## Declaration of competing interest

The authors declare that they have no known competing financial interests or personal relationships that could have appeared to influence the work reported in this paper.

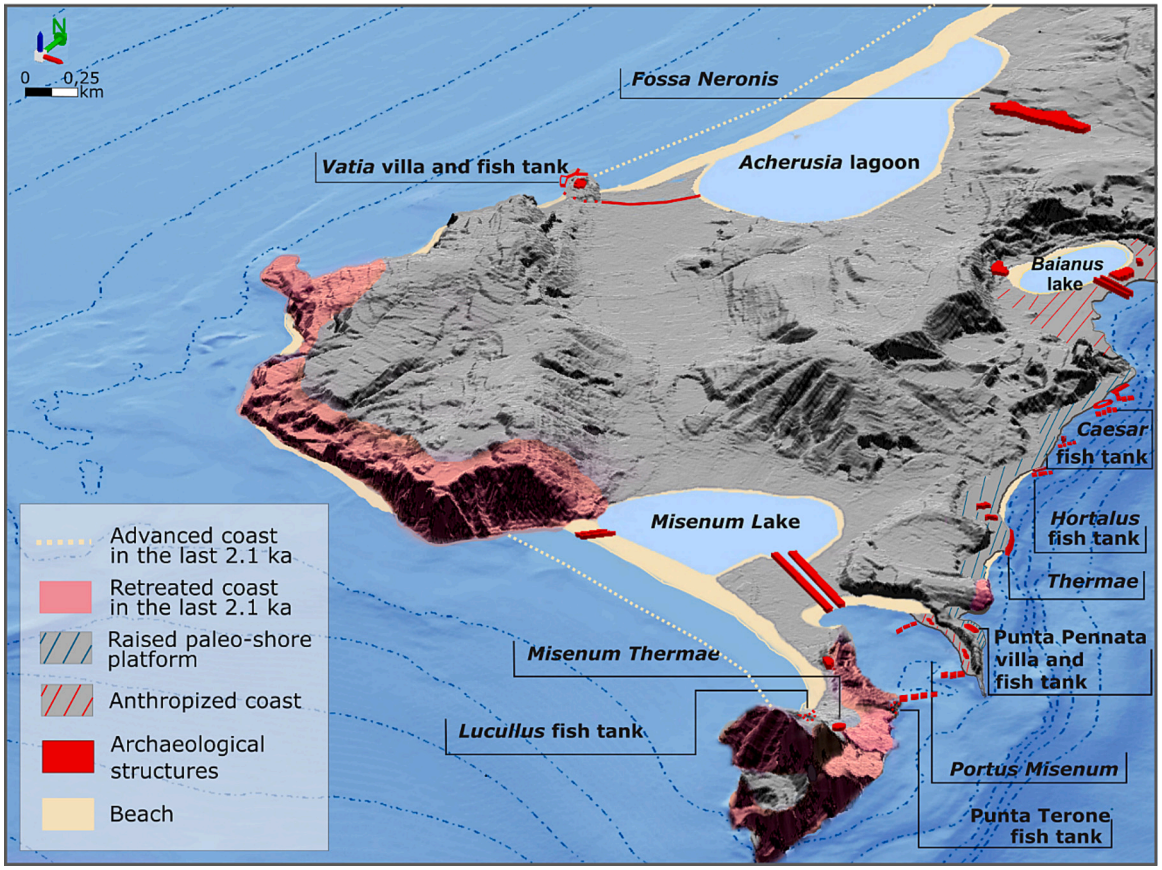


**Fig. 13.** Palaeogeographic scenario between the 1st century BCE and 1st century CE (present-day bathymetry) where the term "anthropized coast" implies a coastal sector mainly modeled by anthropic activities. The basemap was obtained by elaborating LIDAR data provided by the Italian Ministry of Environment.

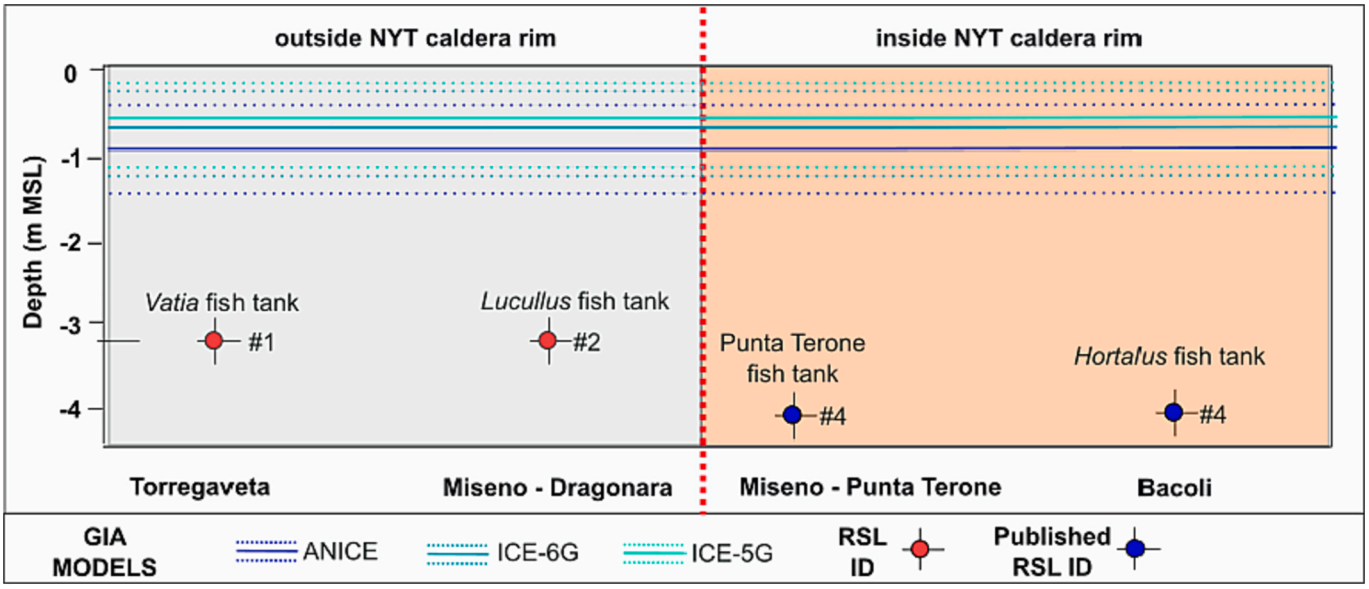


**Fig. 14.** Comparison between the collected RSL data between the inner and outer coastal sector of Campi Flegrei NYT caldera and the GIA models carried out for the study area: ICE-5 G (Peltier, 2004), ICE-6 G (Peltier et al., 2015), and ANICE-SELEN (de Boer et al., 2013, 2014).

## Data availability

Data are available within the article.

## Acknowledgements

The authors sincerely thank Francesco Peluso, Luigi De Luca, and Andrea Gionta for their precious support during the morpho-acoustic marine surveys and Franco Salvatore Ruggiero and Gennaro

Sorrentino of Meno 100 underwater TEK ASD for the highly specialized support during the diving surveys. The coastal LIDAR data used in this paper were kindly provided by the Ministry of the Environment in March 2013. The basemap credits are: Esri, Maxar, GeoEye, Earthstar Geographics, CNES/Airbus DS, USDA, USGS, AeroGRID, IGN, and the GIS User Community. This paper also benefited from the discussion at the Neptune meetings (INQUA CMP project 2003P).

## References

Albert, P.G., Giaccio, B., Isaia, R., Costa, A., Niespolo, E.M., Nomade, S., Pereira, A., Renne, P.R., Hinchliffe, A., Mark, D.F., Brown, R.J., Smith, V.C., 2019. Evidence for a large-magnitude eruption from Campi Flegrei caldera (Italy) at 29 ka. Geology 47 (7), 595–599. https://doi.org/10.1130/G45805.1.

Antonioli, F., D'Orefice, M., Ducci, S., Firmati, M., Foresi, L.M., Graciotti, R., Pantaloni, M., Perazzi, P., Principe, C., 2011. Palaeogeographic reconstruction of northern Tyrrhenian coast using archaeological and geomorphological markers at Pianosa island (Italy). Quat. Int. 232 (1), 31–44. https://doi.org/10.1016/j.quaint.2010.03.017.

Antonioli, F., Anzidei, M., Lambeck, K., Auriemma, R., Gaddi, D., Furlani, S., Orrù, P., Solinas, E., Gaspari, A., Karinja, S., Kovačić, V., Surace, L., 2007. Sea-level change during the Holocene in Sardinia and in the northeastern Adriatic (central Mediterranean Sea) from archaeological and geomorphological data. Quat. Sci. Rev. 26 (19) https://doi.org/10.1016/j.quascirev.2007.06.022.

Ascione, A., Aucelli, P.P.C., Cinque, A., Di Paola, G., Mattei, G., Ruello, M., Russo Ermolli, E., Santangelo, N., Valente, E., 2020. Geomorphology of Naples and the Campi Flegrei: human and natural landscapes in a restless land. J. Maps 17 (2), 1–11. https://doi.org/10.1080/17445647.2020.1768448.

Aucelli, P., Cinque, A., Mattei, G., Pappone, G., 2016. Historical sea level changes and effects on the coasts of Sorrento Peninsula (Gulf of Naples): new constrains from recent geoarchaeological investigations. Palaeogeogr. Palaeoclimatol. Palaeoecol. 463, 112–125. https://doi.org/10.1016/j.palaeo.2016.09.022.

Aucelli, P.P.C., Cinque, A., Mattei, G., Pappone, G., 2017a. Late Holocene landscape evolution of the gulf of Naples (Italy) inferred from geoarchaeological data. J. Maps 13 (2), 300–310. https://doi.org/10.1080/17445647.2017.1300611.

Aucelli, P., Brancaccio, L., Cinque, A., 2017b. Vesuvius and Campi Flegrei volcanoes. Activity, landforms and impact on settlements. In: Soldati, M., Marchetti, M. (Eds.), Landscapes and Landforms of Italy. Springer International Publishing, Cham, Switzerland, pp. 389–398. https://doi.org/10.1007/978-3-319-26194-2_33.

Aucelli, P.P.C., Cinque, A., Mattei, G., Pappone, G., Stefanile, M., 2018. Coastal landscape evolution of Naples (Southern Italy) since the Roman period from archaeological and geomorphological data at Palazzo degli Spiriti site. Quat. Int. 483, 23–38. https://doi.org/10.1016/j.quaint.2017.12.040.

Aucelli, P.P.C., Cinque, A., Mattei, G., Pappone, G., Rizzo, A., 2019. Studying relative sea level change and correlative adaptation of coastal structures on submerged Roman time ruins nearby Naples (southern Italy). Quat. Int. 501, 328–348. https://doi.org/10.1016/j.quaint.2017.10.011.

Aucelli, P.P.C., Mattei, G., Caporizzo, C., Cinque, A., Troisi, S., Peluso, F., Stefanile, M., Pappone, G., 2020. Ancient coastal changes due to ground movements and human interventions in the Roman Portus Julius (Pozzuoli Gulf, Italy): results from photogrammetric and direct surveys. Water 12 (3), 658. https://doi.org/10.3390/w12030658.

Aucelli, P.P.C., Mattei, G., Caporizzo, C., Cinque, A., Amato, L., Stefanile, M., Pappone, G., 2021. Multi-proxy analysis of relative sea-level and palaeoshoreline changes during the last 2300 years in the Campi Flegrei caldera, Southern Italy. Quat. Int. 602, 110–130. https://doi.org/10.1016/j.quaint.2021.03.039.

Auriemma, R., Solinas, E., 2009. Archaeological remains as sea level change markers: a review. Quat. Int. 206 (1), 134–146. https://doi.org/10.1016/j.quaint.2008.11.012.

Bellucci, F., Woo, J., Kilburn, C.R., Rolandi, G., 2006. Ground deformation at Campi Flegrei, Italy: implications for hazard assessment. Geol. Soc. Lond. Spec. Publ. 269, 141–157.

Benini, A., 2007. Il porto e la peschiera di Miseno (NA): nuovi dati archeologici per lo studio delle variazioni del livello del mare nell'area flegrea. In: Atti del Convegno Internazionale di Studi. Trieste, 8-10 novembre 2007.

Benini, A., Lanterni, L., 2010. Il porto romano di Misenum: nuove acquisizioni. In: Blackman, D.J., Lentini, M.C. (Eds.), Ricoveri per navi militari nei porti del Mediterraneo antico e medievale. Atti del Workshop (Ravello 2005), pp. 109–116. Edipuglia, Bari.

Benini, A., Ferrari, G., Lamagna, R., 2008. Le peschiere di Lucullo (Miseno-Napoli). In: Atti VI Convegno Nazionale di Speleologia in Cavità Artificiali - OPERA IPOGEA 1/2; 30 maggio - 2 giugno, Napoli, IT, pp. 159–168.

de Boer, B., van de Wal, R.S.W., Lourens, L.J., Bintanja, R., 2013. A continuous simulation of global ice volume over the past 1 million years with 3-D ice-sheet models. Clim. Dyn. 41, 1365–1384. https://doi.org/10.1007/s00382-012-1562-2.

de Boer, B., Stocchi, P., Van De Wal, R., 2014. A fully coupled 3-D ice-sheet-sea-level model: algorithm and applications. Geosci. Model Dev. 7, 2141–2156. https://doi.org/10.5194/gmd-7-2141-2014.

Borriello, M., d'Ambrosio, A., 1979. Baiae-Misenum (Forma Italiae regio I, XIV). Olschki, Florence, p. 179. https://doi.org/10.2307/299593.

Brun, J.P., Morhange, C., Munzi, P., Stefaniuk, L., 2002. L'evoluzione dell'ambiente nei Campi Flegrei e le sue implicazioni storiche: il caso di Cuma e le ricerche del Centre Jean Bérard nella laguna di Licola. In: Ambiente e paesaggio nella Magna Grecia, 42, pp. 397–435 (ISAMG-Istituto per la storia e l'archeologia della Magna Grecia).

Budillon, F., Amodio, S., Contestabile, P., Alberico, I., Innangi, S., Molisso, F., 2020. The present-day nearshore submarine depositional terraces off the Campania coast (South-eastern Tyrrhenian Sea): An analysis of their morpho-bathymetric variability. In: Proceedings. MetroSea 2020 IMEKO -TC19 International Workshop on Metrology for the Sea, Naples, Italy, pp. 132–138.

Budillon, F., Amodio, S., Alberico, I., Contestabile, P., Vacchi, M., Innangi, S., Molisso, F., 2022. Present-day infralittoral prograding wedges (IPWs) in Central-Eastern Tyrrhenian Sea: critical issues and challenges to their use as geomorphological indicators of sea level. Mar. Geol. 450, 106821 https://doi.org/10.1016/j.margeo.2022.106821.

Caporizzo, C., Gracia, F.J., Aucelli, P.P.C., Barbero, L., Martín-Puertas, C., Lagóstena, L., Ruiz, J.A., Alonso, C., Mattei, G., Galán-Ruffoni, I., López-Ramírez, J.A., Higueras-Milena, A., 2021a. Late-Holocene evolution of the Northern Bay of Cádiz from geomorphological, stratigraphic and archaeological data. Quat. Int. 602, 92–109. https://doi.org/10.1016/j.quaint.2021.03.028.

Caporizzo, C., Aucelli, P.P.C., Di Martino, G., Mattei, G., Tonielli, R., Pappone, G., 2021b. Geomorphometric analysis of the natural and anthropogenic seascape of Naples (Italy): A high-resolution morpho-bathymetric survey. Trans GIS 25, 2571–2595. https://doi.org/10.1111/tgis.12829.

Caputo, P., 2006. Ricerche sul suburbio meridionale di Cuma. Ricerche sul suburbio meridionale di Cuma, pp. 107–134.

Chiodini, G., Caliro, S., Avino, R., Bagnato, E., Capecchiacci, F., Carandente, A., Cardellini, C., Minopoli, C., Tamburello, G., Tripaldi, S., Aiuppa, A., 2022. The hydrothermal system of the Campi Flegrei Caldera, Italy. In: Campi Flegrei. Springer, Berlin, Heidelberg, pp. 239–255.

Ciaramella, A., Perrotta, F., Pappone, G., Aucelli, P., Peluso, F., Mattei, G., 2021. Environment object detection for marine ARGO drone by deep learning. In: Pattern Recognition. ICPR International Workshops and Challenges. ICPR 2021. Lecture Notes in Computer Science 12666. Springer, Cham. https://doi.org/10.1007/978-3-030-68780-9_12.

Cinque, A., Russo, F., Pagano, M., 1991. La successione dei terreni di età post-Romana delle Terme di Miseno (Napoli): nuovi dati per la storia e la stratigrafia del bradisisma puteolano. Boll. Soc. Geol. Ital. 110, 231–244.

Cinque, A., Aucelli, P.P.C., Brancaccio, L., Mele, R., Milia, A., Robustelli, G., Romano, P., Russo, F., Russo, M., Santangelo, N., Sgambati, D., 1997. Volcanism, tectonics and recent geomorphological change in the Bay of Napoli. Geogr. Fis. Din. Quat. 3 (2), 123–141.

Cinque, A., Irollo, G., Romano, P., Ruello, M.R., Amato, L., Giampaola, D., 2011. Ground movements and sea level changes in urban areas: 5000 years of geological and archaeological record from Naples (Southern Italy). Quat. Int. 232 (1–2), 45–55. https://doi.org/10.1016/j.quaint.2010.06.027.

Cocco, E., Iacono, Y., Iuliano, S., Lista, M.R., 2002. Lineamenti morfodinamici e sedimentari del litorale dei Campi Flegrei (Campania, Italia Meridionale). Il Quaternario, Ital. J. Quat. Sci. 15 (2), 209–220.

D'Antonio, M., Civetta, L., Orsi, G., Pappalardo, L., Piochi, M., Caradente, A., de Vita, S., Di Vito, M.A., Isaia, R., 1999. The present state of the magmatic system of the Campi Flegrei caldera based on a reconstruction of its behavior in the past 12 Ka. J. Volcanol. Geotherm. Res. 91, 247–268. https://doi.org/10.1016/S0377-0273(99)00038-4.

D'Arms, J.B., 1970. Romans on the Bay of Naples: A Social and Cultural Study of the Villas and Their Owners From 150 B.C. to A.D. 400. Harvard University Press, Cambridge, UK, pp. 1–100.

De Pippo, T., Donadio, C., Pennetta, M., Terlizzi, F., Vecchione, C., Vegliante, M., 2002. Seabed morphology and pollution along the Bagnoli coast (Naples, Italy): A hypothesis for environmental restoration. Mar. Ecol. 23, 154–168. https://doi.org/10.1111/j.1439-0485.2002.tb00015.x.

De Pippo, T., Donadio, C., Pennetta, M., Terlizzi, F., Valente, A., 2007. Genesis and morphological evolution of Fusàro lagoon (Campania, southern Italy) in the Holocene. Boll. Soc. Geol. Ital. 126 (1), 89.

De Vivo, B., 2006. Volcanism in the Campania Plain: Vesuvius, vol. 9 (Campi Flegrei and Ignimbrites Elsevier).

Deino, A.L., Orsi, G., Piochi, M., de Vita, S., 2004. The age of the Neapolitan Yellow Tuff caldera-forming eruption (Campi Flegrei caldera-Italy) assessed by 40Ar/39Ar dating method. J. Volcanol. Geotherm. Res. 185, 48–56. https://doi.org/10.1016/S0377-0273(03)00396-2.

Del Gaudio, C., Aquino, I., Ricciardi, G.P., Ricco, C., Scandone, R., 2010. Unrest episodes at Campi Flegrei: a reconstruction of vertical ground movements during 1905–2009. J. Volcanol. Geotherm. Res. 195 (1), 48–56. https://doi.org/10.1016/j.jvolgeores.2010.05.014.

Di Donato, V., Ruello, M.R., Liuzza, V., Carsana, V., Giampaola, D., Di Vito, M.A., Morhange, C., Cinque, A., Russo Ermolli, E., 2018. Development and decline of the ancient harbor of Neapolis. Geoarcheaology 33 (4), 542–557. https://doi.org/10.1002/gea.21673.

Di Fraia, G., 2013. Bauli: Storia e Monumenti. Ed. Freebacoli, Bacoli, IT.

Di Vito, A., Acocella, V., Aiello, G., Barra, D., Battaglia, M., Carandente, A., Del Gaudio, C., de Vita, S., Ricciardi, G.P., Ricco, C., Scandone, R., Terrasi, F., 2016. Magma transfer at Campi Flegrei caldera (Italy) before the 1538 AD eruption. Sci. Rep. 6, 32245 https://doi.org/10.1038/srep32245.

Di Vito, M.A., Isaia, R., Orsi, G., Southon, J., de Vita, S., D'Antonio, M., Pappalardo, L., Piochi, M., 1999. Volcanism and deformation since 12,000 years at the Campi Flegrei caldera (Italy). J. Volcanol. Geotherm. Res. 91, 221–246. https://doi.org/10.1016/S0377-0273(99)00037-2.

Dvorak, J.J., Mastrolorenzo, G., 1991. The Mechanisms of Recent Vertical Crustal Movements in Campi Flegrei Caldera, Southern Italy. In: The Geological Society of America Spec. Pap.: Boulder, USA, vol. 263, p. 49.

Engelhart, S.E., Horton, B.P., Douglas, B.C., Peltier, W.R., Tornqvist, T.E., 2009. Spatial variability of late Holocene and 20th century sea-level rise along the Atlantic coast of the United States. Geology 37, 1115–1118. https://doi.org/10.1130/G30360A.1.

Evelpidou, N., Pirazzoli, P., Vassilopoulos, A., Spada, G., Ruggieri, G., Tomasin, A., 2012. Late Holocene sea level reconstructions based on observations of Roman fish tanks, Tyrrhenian Coast of Italy. Geoarchaeology 27 (3), 259–277.

Fedi, M., Cella, F., D'Antonio, M., Florio, G., Paoletti, V., Morra, V., 2018. Gravity modeling finds a large magma body in the deep crust below the Gulf of Naples, Italy. Sci. Rep. 8 (1), 1–19. https://doi.org/10.1038/s41598-018-26346-z.

Ferentinos, G., Fakiris, E., Christodoulou, D., Geraga, M., Dimas, X., Georgiou, N., Kordella, S., Papatheodorou, G., Prevenios, M., Sotiropoulos, M., 2020. Optimal sidescan sonar and subbottom profiler surveying of ancient wrecks: the 'Fiskardo' wreck, Kefallinia Island, Ionian Sea. J. Archaeol. Sci. 113, 105032 https://doi.org/10.1016/j.jas.2019.105032.

Galili, E., Zviely, D., Weinstein-Evron, M., 2005. Holocene sea-level changes and landscape evolution on the northern Carmel coast (Israel). Méditerranée. Revue géographique des pays méditerranéens. J. Mediterr. Geogr. 104, 79–86.

Georgiou, N., Dimas, X., Papatheodorou, G., 2021. Integrated methodological approach for the documentation of marine priority habitats and submerged antiquities: examples from the Saronic Gulf, Greece. Sustainability 13 (21), 12327. https://doi.org/10.3390/su132112327.

Giordano, F., 1995. Marine Geophysical Methods for archaeological investigation of volcanic and bradyseismic areas. In: Annals of Geophysics XXXVIII, 5–6. November–December 1995.

Gunther, R.T., 1913. Pausilypon the Imperial Villa Near Naples. Oxford University Press.

Iliano, G., 2017. Misenum: the harbour and the city. Landscapes in context. Archeol. Calc. 28 (2), 379–389.

Isaia, R., Iannuzzi, E., Sbrana, A., Marianelli, P., 2016. Note Illustrative della Carta Geologica d'Italia alla scala 1: 50.000, Foglio 446–447 Napoli (aree emerse).

Isaia, R., Vitale, S., Marturano, A., Aiello, G., Barra, D., Ciarcia, S., Iannuzzi, E., Tramparulo, F., 2019. High-resolution geological investigations to reconstruct the long-term ground movements in the last 15 kyr at Campi Flegrei caldera (southern Italy). J. Volcanol. Geotherm. Res. 385, 143–158. https://doi.org/10.1016/j.jvolgeores.2019.07.012.

Kennedy, B.M., Holohan, E.P., Stix, J., Gravley, D.M., Davidson, J.R., Cole, J.W., Burchardt, S., 2018. Volcanic and Igneous Plumbing Systems of Caldera Volcanoes. In: Volcanic and Igneous Plumbing Systems. Elsevier, pp. 259–284.

Lafon, X., 2001. Villa Marina: Recherches sur les villas littorales de l'Italie romaine (IIIe: siècle av JC-IIIe siè), 307. École Française de Rome, pp. 507–520.

Lambeck, K., Anzidei, M., Antonioli, F., Benini, A., Esposito, A., 2004. Sea level in Roman time in the Central Mediterranean and implications for recent change. Earth Planet. Sci. Lett. 224 (3–4), 563–575. https://doi.org/10.1016/j.epsl.2004.05.031.

Lambeck, K., Anzidei, M., Antonioli, F., Benini, A., Verrubbi, V., 2018. Tyrrhenian sea level at 2000 BP: evidence from Roman age fish tanks and their geological calibration. Rend. Lincei Sci. Fis. Nat. 29, 69–80. https://doi.org/10.1007/s12210-018-0715-6.

Leoni, G., Dai Pra, G., 1997. Variazioni del livello del mare nel tardo olocene, ultimi 2500 anni, lungo la costa del Lazio in base ad indicatori geo-archeologici: interazioni fra neotettonica, eustatismo e clima. ENEA, Unità comunicazione e informazione.

Lorscheid, T., Stocchi, P., Casella, E., Gómez-Pujol, L., Vacchi, M., Mann, T., Rovere, A., 2017. Paleo sea-level changes and relative sea-level indicators: precise measurements, indicative meaning and glacial isostatic adjustment perspectives from Mallorca (Western Mediterranean). Palaeogeogr. Palaeoclimatol. Palaeoecol. 473, 94–107. https://doi.org/10.1016/j.palaeo.2017.02.028.

Maiuri, A., 1963. I Campi Flegrei. Libreria dello Stato, Roma.

Maiuri, A., 1983. Itinerario Flegreo. Bibliopolis, Napoli.

Marino, C., Ferranti, L., Natale, J., Anzidei, M., Benini, A., Sacchi, M., 2022. Quantitative reconstruction of Holocene ground displacements in the offshore part of the Campi Flegrei caldera (southern Italy): Perspectives from seismo-stratigraphic and archaeological data. Mar. Geol. 447, 106797 https://doi.org/10.1016/j.margeo.2022.106797.

Mattei, G., Troisi, S., Aucelli, P.P.C., Pappone, G., Peluso, F., Stefanile, M., 2018a. Sensing the submerged landscape of Nisida Roman Harbour in the Gulf of Naples from integrated measurements on a USV. Water 10 (11), 1686. https://doi.org/10.3390/w10111686.

Mattei, G., Troisi, S., Aucelli, P.P.C., Pappone, G., Peluso, F., Stefanile, M., 2018b. Multiscale reconstruction of natural and archaeological underwater landscape by optical and acoustic sensors. In: Proceedings of the 2018 IEEE International Workshop on Metrology for the Sea; Learning to Measure Sea Health Parameters (MetroSea), Bari, Italy, 8–10 October, pp. 46–49.

Mattei, G., Aucelli, P.P.C., Caporizzo, C., Rizzo, A., Pappone, G., 2020. New geomorphological and historical elements on morpho-evolutive trends and relative sea-level changes of Naples Coast in the last 6000 years. Water 12, 2651. https://doi.org/10.3390/w12092651.

Mattei, G., Caporizzo, C., Corrado, G., Vacchi, M., Stocchi, P., Pappone, G., Schiattarella, M., Aucelli, P.P.C., 2022. On the influence of vertical ground movements on Late-Quaternary sea-level records. A comprehensive assessment along the mid- Tyrrhenian coast of Italy (Mediterranean Sea). Quat. Sci. Rev. 279, 107384 https://doi.org/10.1016/j.quascirev.2022.107384.

Menna, F., Nocerino, E., Troisi, S., Remondino, F., 2015. Joint alignment of underwater and above-the-water photogrammetric 3D models by independent models adjustment. In: The International Archives of the Photogrammetry, Remote Sensing and Spatial Information Sciences, Volume XL-5/W5, Underwater 3D Recording and Modeling, 16–17 April 2015. Sorrento, Italy, Piano di.

Milia, A., Torrente, M.M., Russo, M., Zuppetta, A., 2003. Tectonics and crustal structure of the Campania continental margin: relationships with volcanism. Mineral. Petrol. 79, 33–47. https://doi.org/10.1007/s00710-003-0005-5.

Morhange, C., Marriner, N., 2015. Archeological and biological relative sea-level indicators. In: Shennan, I., Long, A.J., Horton, B.P. (Eds.), Handbook of Sea-Level Research, pp. 146–156. https://doi.org/10.1002/9781118452547.ch9.

Morhange, C., Bourcier, M., Laborel, J., Giallanella, C., Goiran, J.P., Crimaco, L., Vecchi, L., 1999. New data on historical relative sea level movements in Pozzuoli, Phlaegrean Fields, southern Italy. Phys. Chem. Earth, Part A: Solid Earth Geodesy 24 (4), 349–354. https://doi.org/10.1016/S1464-1895(99)00040-X.

Morhange, C., Marriner, N., Laborel, J., Todesco, M., Oberlin, C., 2006. Rapid sea-level movements and non-eruptive crustal deformation in the phlegrean Fields caldera, Italy. Geology 34 (2), 93–96. https://doi.org/10.1130/G21894.1.

Orsi, G., 2022. Volcanic and Deformation History of the Campi Flegrei Volcanic Field, Italy. In: Campi Flegrei. Springer, Berlin, Heidelberg, pp. 1–53. https://doi.org/10.1007/978-3-642-37060-1_1.

Paget, R.F., 1971. From Baiae to Misenum. In: Vergilius, 17, pp. 22–38.

Pappone, G., Aucelli, P.P.C., Mattei, G., Peluso, F., Stefanile, M., Carola, A., 2019. A detailed reconstruction of the Roman landscape and the submerged archaeological structure at "Castel dell'Ovo islet" (Naples, Southern Italy). Geosciences 9, 170. https://doi.org/10.3390/geosciences9040170.

Peltier, W.R., 2004. Global glacial isostasy and the surface of the Ice-Age Earth: the ICE-5G(VM2) model and GRACE. Annu. Rev. Earth Planet. Sci. 32, 111–149. https://doi.org/10.1146/annurev.earth.32.082503.144359.

Peltier, W.R., Argus, D.F., Drummond, R., 2015. Space geodesy constrains ice-age terminal deglaciation: the global ICE-6G_C (VM5a) model. J. Geophys. Res. Solid Earth 120, 450–487. https://doi.org/10.1002/2014JB011176.

Quinn, R., Dean, M., Lawrence, M., Liscoe, S., Boland, D., 2005. Backscatter responses and resolution considerations in archaeological side-scan sonar surveys: a control experiment. J. Archaeol. Sci. 32 (8), 1252–1264. https://doi.org/10.1016/j.jas.2005.03.010.

Romano, P., Di Vito, M.A., Giampaola, D., Cinque, A., Bartoli, C., Boenzi, G., Detta, F., Di Marco, M., Giglio, M., Iodice, S., Liuzza, V., Ruello, M.R., Schiano di Cola, C., 2013. Intersection of exogenous, endogenous and anthropogenic factors in the Holocene landscape: a study of the Naples coastline during the last6000 years. Quat. Int. 303, 107–119. https://doi.org/10.1016/j.quaint.2013.03.031.

Rovere, A., Stocchi, P., Vacchi, M., 2016. Eustatic and relative sea level changes. Curr. Clim. Change Rep. 2 (4), 221–231. https://doi.org/10.1007/s40641-016-0045-7.

Russo Ermolli, E., Romano, P., Ruello, M.R., Lumaga, M.R.B., 2014. The natural and cultural landscape of Naples (southern Italy) during theGraeco-Roman and LateAntique periods. J. Archaeol. Sci. 42, 399–411. https://doi.org/10.3390/geosciences9040170.

Santacroce, R., Cristofolini, R., Volpe, L., Orsi, G., Rosi, M., 2003. Italian active volcanoes. Episodes 26, 227–234.

Scicchitano, G., Antonioli, F., Berlinghieri, E.F.C., Dutton, A., Monaco, C., 2008. Submerged archaeological sites along the Ionian coast of southeastern Sicily (Italy) and implications for the Holocene relative sea-level change. Quat. Res. 70 (1), 26–39. https://doi.org/10.1016/j.yqres.2008.03.008.

Shennan, I., 2015. Handbook of sea-level research: framing research questions. In: Shennan, I., Long, A.J., Horton, B.P. (Eds.), Handbook of Sea-level Research. John Wiley & Sons, Oxford, UK, pp. 3–25. https://doi.org/10.1002/9781118452547.

Shennan, I., Horton, B., 2002. Holocene land- and sea-level changes in Great Britain. J. Quat. Sci. 17 (5–6), 511–526. https://doi.org/10.1002/jqs.710.

Sivan, D., Wdowinski, S., Lambeck, K., Galili, E., Raban, A., 2001. Holocene sea-level changes along the Mediterranean coast of Israel, based on archaeological observations and numerical model. Palaeogeogr. Palaeoclimatol. Palaeoecol. 167 (1–2), 101–117. https://doi.org/10.1016/S0031-0182(00)00234-0.

Smith, V.C., Isaia, R., Pearce, N.J.C., 2011. Tephrostratigraphy and glass compositions of post-15 kyr Campi. Flegrei eruptions: implications for eruption history and chronostratigraphic markers. Quat. Sci. Rev. 30 (25–26), 3638–3660. https://doi.org/10.1016/j.quascirev.2011.07.012.

Soricelli, G., De Rossi, G., Di Giovanni, V., Miniero, P., Salmieri, S., 2010. Il porto di Miseno (Campania-Italia) in età tardonatica: analisi dei contesti ceramici. In: Late Roman Coarse Wares, Cooking Wares and Amphorae in the Mediterranean. Archaeology and archaeometry. Comparison between western and eastern Mediterranean. Archaeopress Publishers of British Archaeological Reports, Oxford, pp. 487–495.

Spada, G., Stocchi, P., 2007. SELEN: a Fortran 90 program for solving the "sea level equation". Comput. Geosci. 33, 538. https://doi.org/10.1016/j.cageo.2006.08.006.

Todesco, M., Chiodini, G., Macedonio, G., 2003. Monitoring and modelling hydrothermal fluid emission at La Solfatara (Phlegrean Fields, Italy). An interdisciplinary approach to the study of diffuse degassing. J. Volcanol. Geotherm. Res. 125, 57–79. https://doi.org/10.1016/S0377-0273(03)00089-1.

Todesco, M., Costa, A., Comastri, A., Colleoni, F., Spada, G., Quareni, F., 2014. Vertical ground displacement at Campi Flegrei (Italy) in the fifth century: rapid subsidence driven by pore pressure drop. Geophys. Res. Lett. 41, 1471–1478.

Troisi, S., Del Pizzo, S., Gaglione, S., Miccio, A., Testa, R.L., 2015. 3D models comparison of complex shell in underwater and dry environments. Int. Arch. Photogramm. Remote Sens. Spat. Inf. Sci. 40, 215–222.

Tursi, M.F., Minervino, Amodio A., Caporizzo, C., Del Pizzo, S., Figliomeni, F.G., Mattei, G., Parente, C., Rosskopf, C.M., Aucelli, P.P.C., 2023. The response of sandstone sea cliffs to holocene sea-level rise by means of remote sensing and direct

surveys: the case study of Punta Licosa Promontory (Southern Italy). Geosciences 13, 120. https://doi.org/10.3390/geosciences13040120.

Vacchi, M., Marriner, N., Morhange, C., Spada, G., Fontana, A., Rovere, A., 2016. Multiproxy assessment of Holocene relative sea-level changes in the western Mediterranean: Sea-level variability and improvements in the definition of the isostatic signal. Earth Sci. Rev. 155, 172–197. https://doi.org/10.1016/j.earscirev.2016.02.002.

Vacchi, M., Russo Ermolli, E., Morhange, C., Ruello, M., Di Donato, V., Di Vito, M., Giampaola, D., Carsana, V., Liuzza, V., Cinque, A., Boetto, G., Poveda, P., Boenzi, G., Marriner, N., 2019. Millennial variability of rates of sea-level rise in the ancient harbour of Naples (Italy, western Mediterranean Sea). Quat. Res. 93, 284–298. https://doi.org/10.1017/qua.2019.60.